







Computational guided approach for drug repurposing against SARS-CoV-2

Jigisha Anand^{*,1} , Tanmay Ghildiyal² , Aakanksha Madhwal² , Rishabh Bhatt² ,
Devvret Verma¹  & Nishant Rai¹ 

¹Department of Biotechnology, Graphic Era (Deemed to be University), Clement Town, Dehradun, Uttarakhand-248001, India

²Department of Life Sciences, Graphic Era (Deemed to be University), Clement Town, Dehradun, Uttarakhand-248001, India

*Author for correspondence: jiggs21@gmail.com

Background: In the current SARS-CoV-2 outbreak, drug repositioning emerges as a promising approach to develop efficient therapeutics in comparison to *de novo* drug development. The present investigation screened 130 US FDA-approved drugs including hypertension, cardiovascular diseases, respiratory tract infections (RTI), antibiotics and antiviral drugs for their inhibitory potential against SARS-CoV-2. **Materials & methods:** The molecular drug targets against SARS-CoV-2 proteins were determined by the iGEM-DOCK computational docking tool. The protein homology models were generated through SWISS Model workspace. The pharmacokinetics of all the ligands was determined by ADMET analysis. **Results:** The study identified 15 potent drugs exhibiting significant inhibitory potential against SARS-CoV-2. **Conclusion:** Our investigation has identified possible repurposed drug candidates to improve the current *modus operandi* of the treatment given to COVID-19 patients.

First draft submitted: 5 December 2020; Accepted for publication: 2 February 2021; Published online: 2 March 2021

Keywords: ADMET • *in silico* • nsp3 • nsp5 • protein modeling • SARS-CoV-2

Coronaviruses (family: *Coronaviridae*) are known to cause a variety of diseases in mammals and birds. Due to their capability of infecting a large array of animal hosts, these viruses can be transmitted between species. SARS outbreak in southern China (2002) and Middle East respiratory syndrome (MERS) outbreak in the Middle East (2012) were both caused by (human) coronaviruses. SARS-CoV-2, another zoonotic (bat-borne), positive sense, ssRNA coronavirus, and a successor of SARS-CoV-1 (SARS outbreak), is responsible for the current COVID-19 crisis [1]. It belongs to the subfamily Orthocoronavirinae; genus *Betacoronavirus* (lineage B) which naturally infects bats and rodents [2–4].

The genome of SARS-CoV-2 consists of seven genes organized into 5' nonstructural protein-coding regions and 3' structural and nonessential accessory protein-coding regions [5]. Gene 1 is organized into two very large open reading frames (1a and 1b), which are translated into replicase consisting of two large polypeptides – pp1a (~400 kDa) and pp1b (~800 kDa). The replicase comprises of protein domain that contains 16 nonstructural protein units indicated by nsp1–nsp16 [6]. These nsp1–nsp16 form double membrane vesicles which is a virion replication and transcription complex [7], while nonstructural protein 3 (nsp3) plays an important role in the virion structure, replication and transcription [8].

Genes 2–7 are translated from subgenomic mRNA which encodes the major viral structural proteins like spike protein (S), envelope protein (E), membrane protein (M), nucleocapsid protein (N) and accessory proteins that are essential for the virus–cell receptor binding. The newly synthesized structural proteins are released into the endoplasmic reticulum. All of these proteins, along with N protein are linked to the viral genomic RNA and localized in the endoplasmic reticulum–golgi intermediate compartment (ERGIC) region from where they are packed in smooth-walled vesicles and released from the cell to infect other cells [9,10].

Consisting of 29,891 nucleotides encoding 9860 amino acids, the SARS-CoV-2 viral genome (26–32 kb) bears 82% similarity to the SARS CoV-1 genome [5]. Spike glycoprotein (S), membrane and envelope glycoproteins (M and E), and N protein are the major structural proteins encoded by this virus [6]. The spike glycoproteins that form

the characteristic corona around the virus, form homodimers that bind to specific cellular receptors in the host via their N-terminus and are highly conserved regions [11]. The M glycoproteins play a pivotal role in helping the virus fusion into the cell, regeneration of virions and production of antigenic proteins [12,13].

The E glycoprotein of SARS-CoV-2 is a small protein composed of approximately 76–109 amino acids. About 30 amino acids in the N-terminal of E proteins allow attachment to the membrane of viruses and play a critical role in the assembly and morphogenesis of virions within the host cell [14,15]. N protein is a multifunctional protein that plays an important role in RNA packaging into nucleocapsid, replication and transcription [13]. This protein has shown 90% amino acid homology with SARS-CoV-2 responsible for causing an epidemic in 2003, and thus is highly conserved, stable and stands as a key target in antiviral drug development against SARS-CoV-2 [16].

The main protease (nsp5, 3CLpro) of SARS-CoV-2 shows the considerable sequence and structural resemblance with the protease of closely related members like SARS-CoV and MERS-CoV while it has dissimilarity with human protease [17]. This protein has a pivotal role in viral gene expression, formation of replication complex through its proteolytic cleavage of replicase polyproteins and induces cell death in uninfected neighboring cells [17–19]. Hence, viral protease is a well-studied SARS-CoV-2 protein and is a validated drug target for the development of novel coronavirus potential inhibitors. The main protease, therefore, could serve as the prime target to inhibit SARS-CoV-2 replication and preventing uncontrolled regulation of signaling cascade in infected cells, which may trigger death in neighboring uninfected cells [19].

The pathogenesis of SARS-CoV-2 initiates with its replication, which occurs in the host cell cytoplasm. The binding of the virus to the ACE-2 receptor on the host cell surface via receptor binding domain of spike (S) protein causes a conformational change in the precursor protein structure and thereby initiates the process of viral invasion in the host cell [20,21]. ACE-2 which is a membrane-bound zinc metalloenzyme and monocarboxypeptidase are found ubiquitously as surface receptor glycoproteins on heart, intestine, kidney and pulmonary alveolar (type II) cells of humans [22,23].

The infection and fatalities in coronavirus disease known as COVID-19 infection (also formerly called as 2019 novel coronavirus) are reportedly higher in individuals with comorbidities like hypertension, diabetes, liver and kidney dysfunctions [24]. This has imposed a challenging situation for health professionals to select appropriate therapeutics for the treatment under limited time for clinical setup and unavailability of new and specific drugs [25,26].

Therefore, because of the increasing numbers of patients with comorbidities and the associated risk factor linked with COVID-19 infections, drug repurposing has received a lot of interest from researchers. Drug repurposing is a process of identifying the novel application of approved drugs; this is feasible and cost-effective compared with the *de novo* drug-discovery mechanism [26,27].

Considering the prospects of repurposed drugs and structural relatedness of SARS-CoV-2 with SARS-CoV and MERS-CoV, we have selected 130 US FDA-approved drugs that have reportedly shown antiviral potentials. The selected drugs have been categorized into three types: antiviral drugs (designated as type-I); anticoagulants, antihypertensive drugs, and drugs against cardiovascular disease and respiratory tract infections (RTIs; designated as type-II); and other miscellaneous antimicrobial agents with prospects for drug repurposing (designated as type-III). Some of these drugs have been previously screened and repurposed for their application as an antiviral drug against SARS-CoV and MERS-CoV [26–28]. All 130 drugs were assessed for their possible inhibitory potential against target SARS-CoV-2 proteins using computational tools. The interaction energies generated via molecular docking study were determined. This study, therefore, provides possible drug repositioning candidates and their targets for future *in vitro* and *in vivo* investigations of SARS-CoV-2 therapeutics.

Experimental study

The course of our study was aimed at making use of *in silico* tools to screen the potential drugs with their inhibitory activity SARS-CoV-2. Based on the role of structural proteins including S, E, N, and nonstructural proteins nsp3(ribose phosphate), nsp5 (main protease), nsp10 and nsp16 (Mtase-methyltransferase) in the life cycle and pathogenesis of the SARS-CoV-2, we have performed their molecular docking with 130 FDA-approved drugs. The interaction of all the drugs and seven proteins were closely examined to identify the potential drug targets and possible novel candidates for drug repurposing in the treatment of COVID-19 infection (Figure 1).

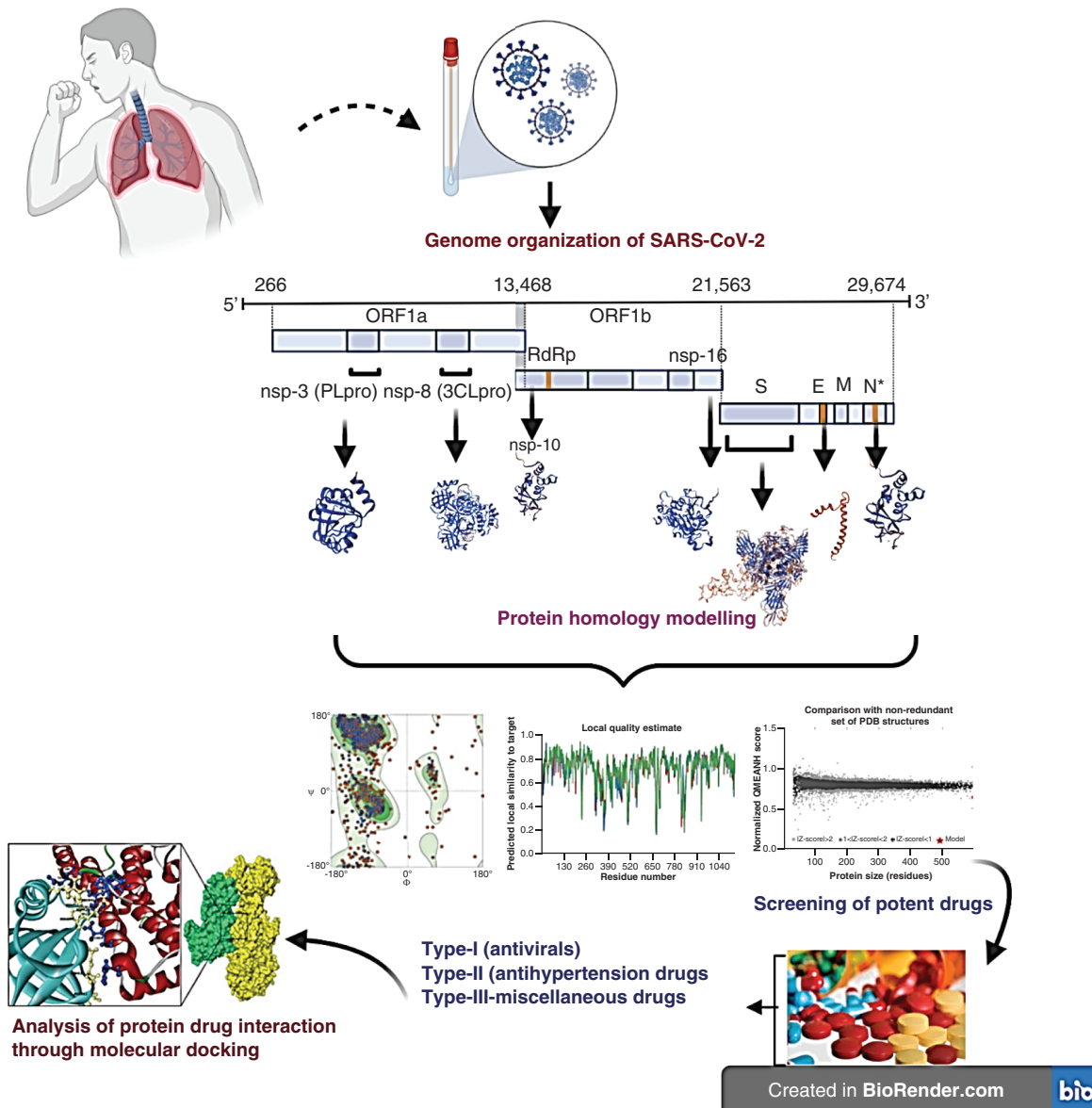


Figure 1. Graphical representation of work plan.

Materials & methods

Retrieval of protein structures

The 3D structure of the structural and nonstructural proteins of SARS-CoV-2 were retrieved in protein data bank (PDB) format (.pdb) using the PHYRE program (Protein Homology/analogy Recognition Engine). The amino acid sequences were derived from the RCSB PDB in a FASTA format (www.rcsb.org/). The physicochemical and functional characterization of proteins was determined using ExPASy's Prot-param server [29]. The 3D-protein homology models were generated from the SWISS MODEL workspace [30,31]. The protein homology models were validated with a Ramachandran plot using the SWISS MODEL workspace. The stereochemical quality of the protein structures was assessed by PROCHECK to evaluate the presence of conserved sequences and related geometry of proteins [32].

Preparation of ligand molecules

The ligand molecules used in the study belong to different classes of medicinal drugs including: antiviral drugs (type-I); anticoagulants, antihypertensive drugs, and drugs against cardiovascular disease and RTIs (type-II); and other

miscellaneous antimicrobial agents (type-III). The code of SMILES for all the aforementioned test molecules was procured from the online chemical database PubChem (<https://pubchem.ncbi.nlm.nih.gov/>) (Tables 1A, 1B & 1C). The 3D structures of the test molecules were then obtained by converting the SMILES code (.smiles format) into PDB (.pdb) format using chemical interconversion software Open Babel (v 2.3.1).

The Drug Likeness reports of all the test molecules were prepared by submitting individual SMILES code for each drug to SwissADME – an omic tool aimed at understanding physicochemical description, pharmacokinetics and drug-like properties of small molecules [33,34]. The toxicity and LD₅₀ of test compounds were analyzed using the admetSAR 2.0 version.

Molecular docking

The binding efficacy of test molecules with the virulent proteins of SARS-CoV-2 was determined by performing docking analysis using iGEMDOCK software (v 2.1), which provides a graphical environment for recognizing pharmacological interactions and virtual screening. The iGEMDOCK generates protein–compound interaction profiles of electrostatic, hydrogen bonding and Van der Waals interactions and infers the pharmacological interactions as well as clusters the screening compounds for the postscreening analysis [35]. On the grounds of evaluated binding energies, it was presumed that how far the drug binds to the target macromolecule. For our study, we used standard docking with a population size of 200, 70 generations and two solutions.

Results

Molecular docking analysis

The 3D structures of the SARS-CoV-2 proteins were generated from the SWISS MODEL workspace. Physicochemical and functional characterization of the SARS-CoV-2 structural and nonstructural proteins was analyzed using ExPASy's Prot-param server (Table 2). The structural templates for protein homology modeling were determined using the SWISS MODEL workspace. The template 6zhg.1.C. with 99.68% of sequence identity was observed for homology modeling of spike glycoproteins, while other protein models showed a 100% sequence identity with their respective templates (Table 3).

The Ramachandran plot depicted structural stability and showed confirmation of residues in the favorable region (Supplementary Figure 1 & Supplementary Table 3). A Ramachandran phi-psi plot for all the seven proteins revealed 88.06–99.40% residues in the allowed region (light grey), and only 0.17–2.06% lay in the disallowed region (white). The above analysis of the predicted structure provides supporting evidence that suggests the predicted 3D structures of SARS-CoV-2 are significant for the docking study. The protein models showed local similarity to the crystal structures of target templates (Supplementary Figure 2). The Q-mean value of protein models was reliable as depicted in the protein homology analysis (Supplementary Figure 3).

The molecular docking using iGEMDOCK generated the binding energies of interaction between ligands and the structural PDB proteins of SARS-CoV-2 (Tables 4A, 4B & 4C). The inhibitory potential of all the drugs was assessed based on the binding energy of their interaction with respective proteins (Figure 2A, B, C & D). The favorable docking sites for the interaction between ligands and SARS-CoV-2 proteins were depicted by AADS (Supplementary Table 1).

ADMET analysis

ADMET parameters, namely 'absorption', 'distribution', 'metabolism' and 'excretion', pharmacokinetic properties, and the drug disposition within an organism were determined using Swiss ADME. The LD₅₀ dose of all the compounds was estimated by the admetSAR 2.0 version, which is a useful tool for *in silico* screening of ADMET profiles of drug candidates and environmental chemicals.

The ADMET analysis showed moderate to high solubility and gastrointestinal (GI) absorption of antiviral drugs, while baloxavir marboxil, danoprevir and sofosbuvir were found to be soluble but exhibit low GI absorption. Out of 58 drugs studied in the type-II category, fosinopril, telmisartan, amiodarone and azithromycin showed poor solubility and low GI absorption. However, their docking analysis revealed favorable molecular interaction with main protease and nsp10 protein (Supplementary Tables 2A, 2B & 2C). Among the type-III category of drugs, fidaxomicin, micafungin, virginiamycin, tunicamycin, amphotericin B and caspofungin depicted high binding affinity with SARS-CoV-2 main protease, N and E proteins, their ADMET analysis predicted the moderate solubility and low GI absorption.

Table 1A. Type-I drugs used for *in silico* study against virulent proteins of SARS-CoV-2.

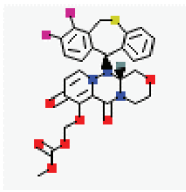
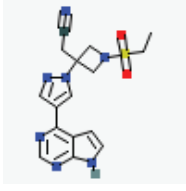
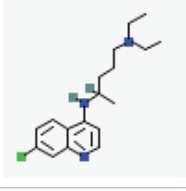
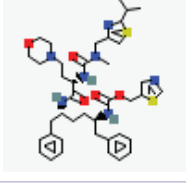
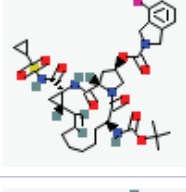
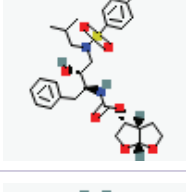
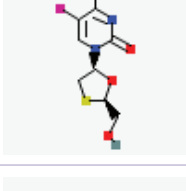
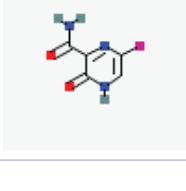
| S. N. | Antiviral drugs | PubChem ID | Molecular formula | Molecular weight | 2D structure |
|-------|--------------------|------------|--------------------------|------------------|---|
| 1. | Baloxavir marboxil | 124081896 | $C_{27}H_{23}F_2N_3O_7S$ | 571.6 g/mol |  |
| 2. | Baricitinib | 244205240 | $C_{16}H_{17}N_7O_2S$ | 371.4 g/mol |  |
| 3. | Chloroquine | 2719 | $C_{18}H_{26}ClN_3$ | 319.9 g/mol |  |
| 4. | Cobicistat | 25151504 | $C_{40}H_{53}N_7O_5S_2$ | 776 g/mol |  |
| 5. | Danoprevir | 11285588 | $C_{35}H_{46}FN_5O_9S$ | 731.8 g/mol |  |
| 6. | Darunavir | 213039 | $C_{27}H_{37}N_3O_7S$ | 547.7 g/mol |  |
| 7. | Emtricitabine | 60877 | $C_8H_{10}FN_3O_3S$ | 247.25 g/mol |  |
| 8. | Favipiravir | 492405 | $C_5H_4FN_3O_2$ | 157.1 g/mol |  |

Table 1A. Type-I drugs used for *in silico* study against virulent proteins of SARS-CoV-2 (cont.).


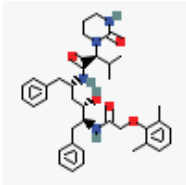
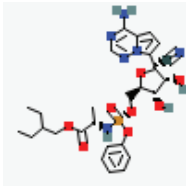
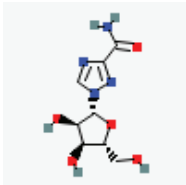
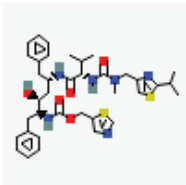
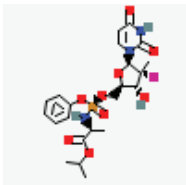
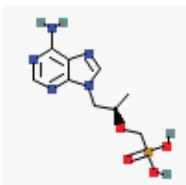
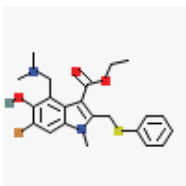
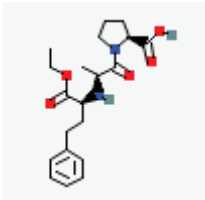
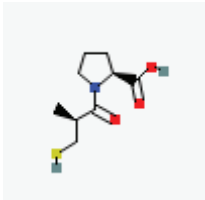
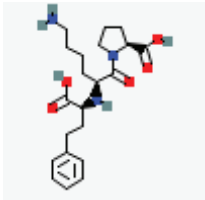
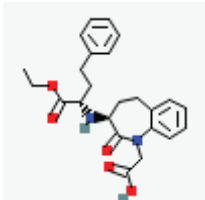
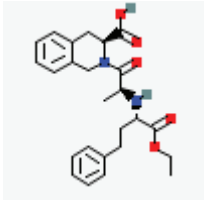
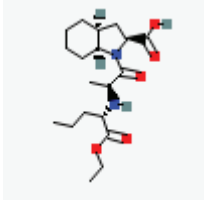
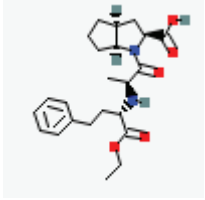
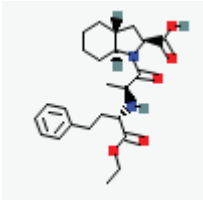
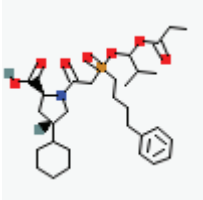
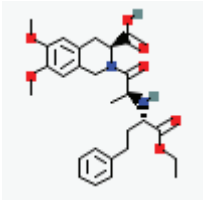
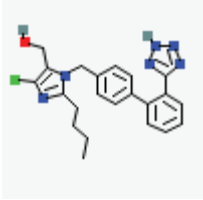
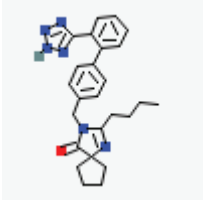
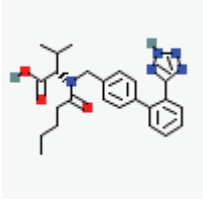
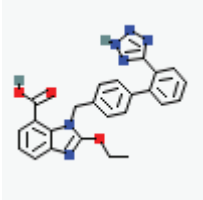
| S. N. | Antiviral drugs | PubChem ID | Molecular formula | Molecular weight | 2D structure |
|-------|----------------------------|------------|-------------------------|------------------|---|
| 9. | Hydroxychloroquine sulfate | 12947 | $C_{18}H_{28}ClN_3O_5S$ | 434 g/mol |  |
| 10. | Lopinavir | 92727 | $C_{37}H_{48}N_4O_5$ | 628.8 g/mol |  |
| 11. | Remdesivir | 121304016 | $C_{27}H_{35}N_6O_8P$ | 602.6 g/mol |  |
| 12. | Ribavirin | 37542 | $C_8H_{12}N_4O_5$ | 244.2 g/mol |  |
| 13. | Ritonavir | 392622 | $C_{37}H_{48}N_6O_5S_2$ | 720.9 g/mol |  |
| 14. | Sofosbuvir | 45375808 | $C_{22}H_{29}FN_3O_9P$ | 529.5 g/mol |  |
| 15. | Tenofovir | 464205 | $C_9H_{14}N_5O_4P$ | 287.21 g/mol |  |
| 16. | Umifenovir | 131411 | $C_{22}H_{25}BrN_2O_3S$ | 477.4 g/mol |  |

Table 1B. Type-II drugs used for *in silico* study against virulent proteins of SARS-CoV-2.

| ACE inhibitors | | | | | |
|----------------|-------------|------------|--|------------------|---|
| S. N. | Compound | PubChem ID | Molecular formula | Molecular weight | 2D structure |
| 1. | Enalapril | 5388962 | C ₂₀ H ₂₈ N ₂ O ₅ | 376.4 g/mol |  |
| 2. | Captopril | 44093 | C ₉ H ₁₅ NO ₃ S | 217.29 g/mol |  |
| 3. | Lisinopril | 5362119 | C ₂₁ H ₃₅ N ₃ O ₇ | 441.5 g/mol |  |
| 4. | Benazepril | 5362124 | C ₅₀ H ₆₀ Cl ₂ N ₄ O ₁₃ S | 1028 g/mol |  |
| 5. | Quinapril | 54892 | C ₂₅ H ₃₀ N ₂ O ₅ | 438.5 g/mol |  |
| 6. | Perindopril | 107807 | C ₁₉ H ₃₂ N ₂ O ₅ | 368.5 g/mol |  |
| 7. | Ramipril | 5362129 | C ₂₃ H ₃₂ N ₂ O ₅ | 416.5 g/mol |  |

ACE: Angiotensin-converting enzyme; RTI: Respiratory tract infection.

Table 1B. Type-II drugs used for *in silico* study against virulent proteins of SARS-CoV-2 (cont.).

| ACE inhibitors | | | | | |
|------------------------------|--------------|------------|----------------------|------------------|---|
| S. N. | Compound | PubChem ID | Molecular formula | Molecular weight | 2D structure |
| 8. | Trandolapril | 5484727 | $C_{24}H_{34}N_2O_5$ | 430.5 g/mol |  |
| 9. | Fosinopril | 23667962 | $C_{30}H_{46}NO_7P$ | 563.7 g/mol |  |
| 10. | Moexipril | 91270 | $C_{27}H_{34}N_2O_7$ | 498.6 g/mol |  |
| Angiotensin receptor-blocker | | | | | |
| S. N. | Compound | PubChem ID | Molecular formula | Molecular weight | 2D structure |
| 1. | Losartan | 11751549 | $C_{22}H_{23}ClN_2O$ | 422.9 g/mol |  |
| 2. | Irbesartan | 3749 | $C_{25}H_{28}N_6O$ | 428.5 g/mol |  |
| 3. | Valsartan | 60846 | $C_{24}H_{29}N_5O_3$ | 435.5 g/mol |  |
| 4. | Candesartan | 2541 | $C_{24}H_{20}N_6O_3$ | 440.5 g/mol |  |

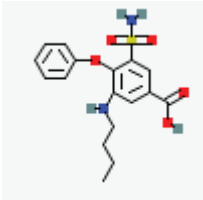
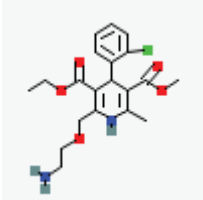
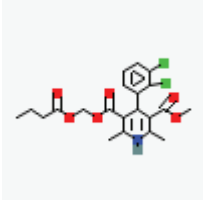
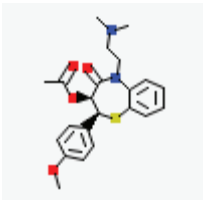
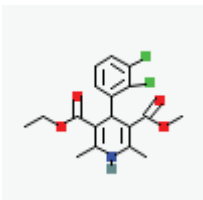
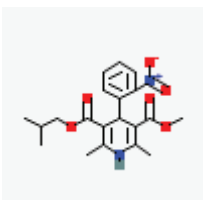
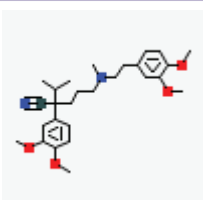
ACE: Angiotensin-converting enzyme; RTI: Respiratory tract infection.

Table 1B. Type-II drugs used for *in silico* study against virulent proteins of SARS-CoV-2 (cont.).

| Angiotensin receptor-blocker | | | | | |
|------------------------------|---------------------|------------|--|------------------|---|
| S. N. | Compound | PubChem ID | Molecular formula | Molecular weight | 2D structure |
| 5. | Olmesartan | 158781 | C ₂₄ H ₂₆ N ₆ O ₃ | 446.5 g/mol |  |
| 6. | Telmisartan | 65999 | C ₃₃ H ₃₀ N ₄ O ₂ | 514.6 g/mol |  |
| 7. | Azilsartan | 135415867 | C ₂₅ H ₂₀ N ₄ O ₅ | 456.4 g/mol |  |
| Diuretics | | | | | |
| S. N. | Compound | PubChem ID | Molecular formula | Molecular weight | 2D structure |
| 1. | Hydrochlorothiazide | 3639 | C ₇ H ₈ ClN ₃ O ₄ S ₂ | 297.7 g/mol |  |
| 2. | Chlorthalidone | 2732 | C ₁₄ H ₁₁ ClN ₂ O ₄ S | 338.8 g/mol |  |
| 3. | Metolazone | 4170 | C ₁₆ H ₁₆ ClN ₃ O ₃ S | 365.8 g/mol |  |
| 4. | Furosemide | 3440 | C ₁₂ H ₁₁ ClN ₂ O ₅ S | 330.74 g/mol |  |

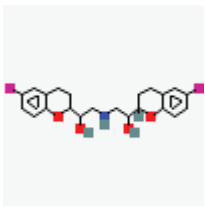
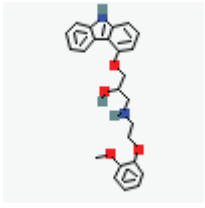
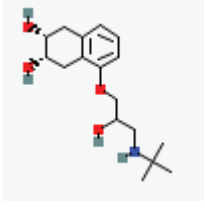
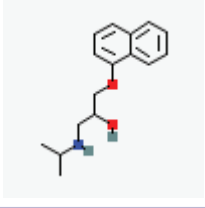
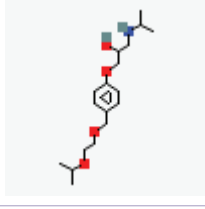
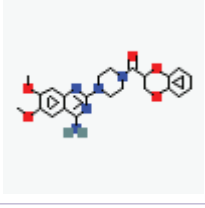
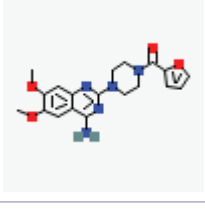
ACE: Angiotensin-converting enzyme; RTI: Respiratory tract infection.

Table 1B. Type-II drugs used for *in silico* study against virulent proteins of SARS-CoV-2 (cont.).

| Diuretics | | | | | |
|--------------------------|-------------|------------|---|------------------|---|
| S. N. | Compound | PubChem ID | Molecular formula | Molecular weight | 2D structure |
| 5. | Bumetanide | 2471 | C ₁₇ H ₂₀ N ₂ O ₅ S | 364.4 g/mol |  |
| Calcium channel blockers | | | | | |
| S. N. | Compound | PubChem ID | Molecular formula | Molecular weight | 2D structure |
| 1. | Amlodipine | 2162 | C ₂₀ H ₂₅ ClN ₂ O ₅ | 408.9 g/mol |  |
| 2. | Clevidipine | 153994 | C ₂₁ H ₂₃ Cl ₂ NO ₆ | 456.3 g/mol |  |
| 3. | Diltiazem | 39186 | C ₂₂ H ₂₆ N ₂ O ₄ S | 414.5 g/mol |  |
| 4. | Felodipine | 3333 | C ₁₈ H ₁₉ Cl ₂ NO ₄ | 384.2 g/mol |  |
| 5. | Nisoldipine | 4499 | C ₂₀ H ₂₄ N ₂ O ₆ | 388.4 g/mol |  |
| 6. | Verapamil | 2520 | C ₂₇ H ₃₈ N ₂ O ₄ | 454.6 g/mol |  |

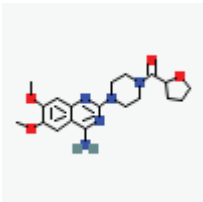
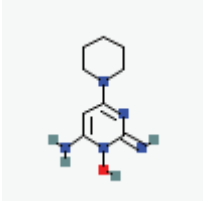
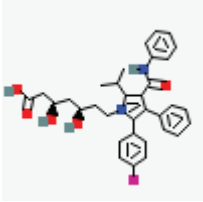
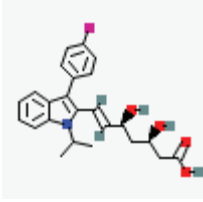
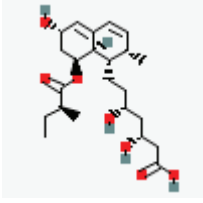
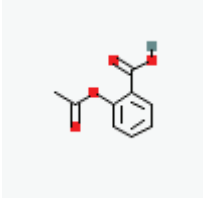
ACE: Angiotensin-converting enzyme; RTI: Respiratory tract infection.

Table 1B. Type-II drugs used for *in silico* study against virulent proteins of SARS-CoV-2 (cont.).

| α -Blockers, β -blockers and vasodilators | | | | | |
|--|-------------|------------|--|------------------|---|
| S. N. | Compound | PubChem ID | Molecular formula | Molecular weight | 2D structure |
| 1. | Nebivolol | 71301 | C ₂₂ H ₂₅ F ₂ NO ₄ | 405.4 g/mol |  |
| 2. | Carvedilol | 2585 | C ₂₄ H ₂₆ N ₂ O ₄ | 406.5 g/mol |  |
| 3. | Nadolol | 39147 | C ₁₇ H ₂₇ NO ₄ | 309.4 g/mol |  |
| 4. | Propranolol | 4946 | C ₁₆ H ₂₁ NO ₂ | 259.339 g/mol |  |
| 5. | Bisoprolol | 2405 | C ₁₈ H ₃₁ NO ₄ | 325.4 g/mol |  |
| 6. | Doxazosin | 3157 | C ₂₃ H ₂₅ N ₅ O ₅ | 451.5 g/mol |  |
| 7. | Prazosin | 4893 | C ₁₉ H ₂₁ N ₅ O ₄ | 383.4 g/mol |  |

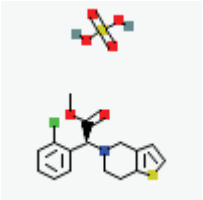
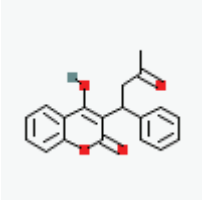
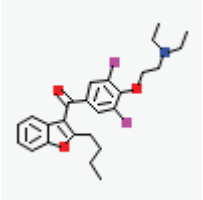
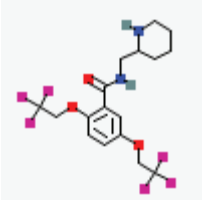
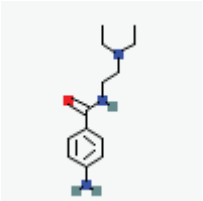
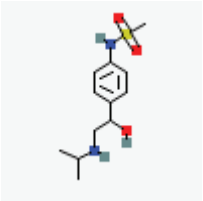
ACE: Angiotensin-converting enzyme; RTI: Respiratory tract infection.

Table 1B. Type-II drugs used for *in silico* study against virulent proteins of SARS-CoV-2 (cont.).

| α-Blockers, β-blockers and vasodilators | | | | | |
|---|--------------|------------|-----------------------|------------------|---|
| S. N. | Compound | PubChem ID | Molecular formula | Molecular weight | 2D structure |
| 8. | Terazosin | 5401 | $C_{19}H_{25}N_5O_4$ | 387.4 g/mol |  |
| 9. | Minoxidil | 4201 | $C_9H_{15}N_5O$ | 209.25 g/mol |  |
| Cardiovascular diseases drugs | | | | | |
| S. N. | Compound | PubChem ID | Molecular formula | Molecular weight | 2D structure |
| 1. | Atorvastatin | 60823 | $C_{33}H_{34}FN_2O_5$ | 557.6 g/mol |  |
| 2. | Fluvastatin | 446155 | $C_{24}H_{26}FNO_4$ | 411.5 g/mol |  |
| 3. | Pravastatin | 4889 | $C_{23}H_{36}O_7$ | 424.5 g/mol |  |
| Anticoagulants and antiplatelet drugs | | | | | |
| S. N. | Compound | PubChem ID | Molecular formula | Molecular weight | 2D structure |
| 1. | Aspirin | 2244 | $C_9H_8O_4$ | 180.16 g/mol |  |

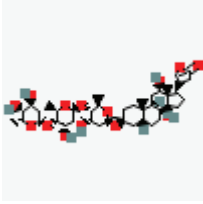
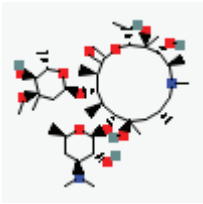
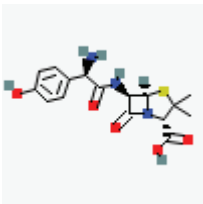
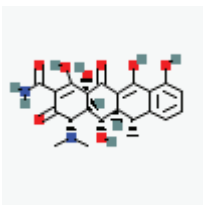
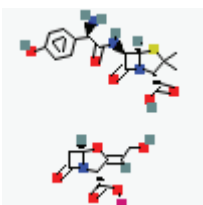
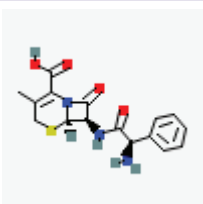
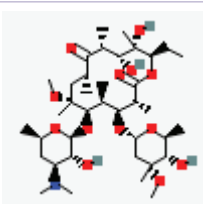
ACE: Angiotensin-converting enzyme; RTI: Respiratory tract infection.

Table 1B. Type-II drugs used for *in silico* study against virulent proteins of SARS-CoV-2 (cont.).

| Anticoagulants and antiplatelet drugs | | | | | |
|---------------------------------------|-----------------------|------------|--|------------------|---|
| S. N. | Compound | PubChem ID | Molecular formula | Molecular weight | 2D structure |
| 2. | Clopidogrel bisulfate | 115366 | C ₁₆ H ₁₈ ClNO ₆ S ₂ | 419.9 g/mol |  |
| 3. | Warfarin | 54678486 | C ₁₉ H ₁₆ O ₄ | 308.3 g/mol |  |
| Anti-arrhythmic drugs | | | | | |
| S. N. | Compound | PubChem ID | Molecular formula | Molecular weight | 2D structure |
| 1. | Amiodarone | 2157 | C ₂₅ H ₂₉ I ₂ NO ₃ | 645.3 g/mol |  |
| 2. | Flecainide | 3356 | C ₁₇ H ₂₀ F ₆ N ₂ O ₃ | 414.34 g/mol |  |
| 3. | Procainamide | 4913 | C ₁₃ H ₂₁ N ₃ O | 235.33 g/mol |  |
| 4. | Sotalol | 5253 | C ₁₂ H ₂₀ N ₂ O ₃ S | 272.37 g/mol |  |

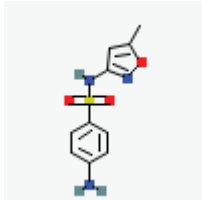
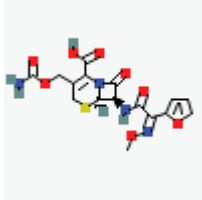
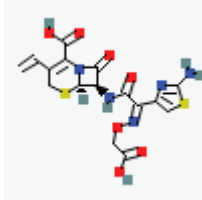
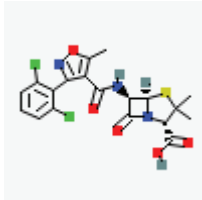
ACE: Angiotensin-converting enzyme; RTI: Respiratory tract infection.

Table 1B. Type-II drugs used for *in silico* study against virulent proteins of SARS-CoV-2 (cont.).

| Cardiac glycosides and drugs used against RTI | | | | | |
|---|----------------|------------|---|------------------|---|
| S. N. | Compound | PubChem ID | Molecular formula | Molecular weight | 2D structure |
| 1. | Digoxin | 2724385 | C ₄₁ H ₆₄ O ₁₄ | 780.9 g/mol |  |
| 2. | Azithromycin | 447043 | C ₃₈ H ₇₂ N ₂ O ₁₂ | 749 g/mol |  |
| 3. | Amoxicillin | 33613 | C ₁₆ H ₁₉ N ₃ O ₅ S | 365.4 g/mol |  |
| 4. | Doxycycline | 54684461 | C ₂₂ H ₂₄ N ₂ O ₈ | 444.4 g/mol |  |
| 5. | Augmentin | 23665637 | C ₂₄ H ₂₇ KN ₄ O ₁₀ S | 602.7 g/mol |  |
| 6. | Cephalexin | 27447 | C ₁₆ H ₁₇ N ₃ O ₄ S | 347.4 g/mol |  |
| 7. | Clarithromycin | 84029 | C ₃₈ H ₆₉ NO ₁₃ | 748 g/mol |  |

ACE: Angiotensin-converting enzyme; RTI: Respiratory tract infection.

Table 1B. Type-II drugs used for *in silico* study against virulent proteins of SARS-CoV-2 (cont.).

| Cardiac glycosides and drugs used against RTI | | | | | |
|---|------------------|------------|---|------------------|--|
| S. N. | Compound | PubChem ID | Molecular formula | Molecular weight | 2D structure |
| 8. | Sulfamethoxazole | 358641 | C ₁₀ H ₁₁ N ₃ O ₃ S | 253.28 g/mol |  |
| 9. | Cefuroxime | 5479529 | C ₁₆ H ₁₆ N ₄ O ₈ S | 424.4 g/mol |  |
| 10. | Cefixime | 5362065 | C ₁₆ H ₁₅ N ₅ O ₇ S ₂ | 453.5 g/mol |  |
| 11. | Dicloxacillin | 18381 | C ₁₉ H ₁₇ Cl ₂ N ₃ O ₅ S | 470.3 g/mol |  |

ACE: Angiotensin-converting enzyme; RTI: Respiratory tract infection.

The lipophilicity of the investigated drugs was indicated between -9.31 and +9.3, except for butenafine hydrochloride (Log $p = 0$). An *in silico* drug likeliness analysis showed that most of the investigated drugs showed an agreement to the Lipinski, Ghose, Veber, Egan and Muegge rules (Supplementary Tables 2A, 2B & 2C).

The study predicted the bioavailability of drugs based on the ADMET score, which was evaluated between 0.11 and 0.56. The admetSAR 2.0 server was used to predict the rat acute toxicity or LD₅₀ value in mol/kg body weight. The study indicated that all the drugs tested against SARS-CoV-2 proteins have LD₅₀ values ranged between 0.17 and 4.42 mol/kg (Supplementary Tables 3A, 3B & 3C).

Discussion

SARS-CoV-2 has emerged as the causal virus for the ongoing COVID-19 pandemic that has spread worldwide. Currently, the cure for COVID-19 is still under trial or observation and multiple researches are ongoing globally to develop a promising vaccine or an antiviral drug. Several drugs like remdesivir and hydroxychloroquine have shown promising results in the treatment of COVID-19 and many more drugs are still under clinical trials. In the current scenario where a completely effective and specific vaccine or drug is still lacking, repurposed drugs could open a new gateway in developing an effective alternative to combat SARS-CoV-2 infection [36].

The SARS-CoV-2 protease is an appealing and important drug target due to its potential involvement in the invasion and replication of the virus. In our study, 15 antiviral drugs with recognized inhibitory potential against different viruses were investigated for their inhibitory activity against SARS-CoV-2. Remdesivir, chloroquine and hydroxychloroquine have been identified as strong inhibitors of the main protease. These drugs are recognized by the WHO among the four potent means of therapeutics against SARS-CoV-2 during the current COVID-19 pandemic [37]. It has been proposed that chloroquine and hydroxychloroquine could alter the endosomal pH and

Table 1C. Type-III drugs used for *in silico* study against virulent proteins of SARS-CoV-2.

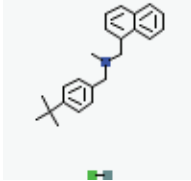
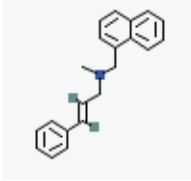
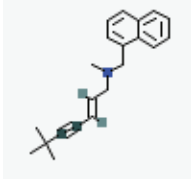
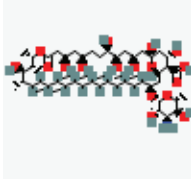
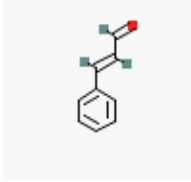
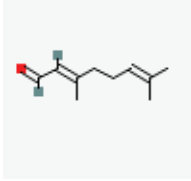


| S. N. | Compound | PubChem ID | Molecular formula | Molecular weight | 2D structure |
|-------|--------------------------|------------|--|------------------|---|
| 1. | Butenafine hydrochloride | 443867 | C ₂₃ H ₂₈ ClN | 353.9 g/mol |  |
| 2. | Naftifine | 47641 | C ₂₁ H ₂₁ N | 287.4 g/mol |  |
| 3. | Terbinafine | 1549008 | C ₂₁ H ₂₅ N | 291.4 g/mol |  |
| 4. | Amphotericin B | 5280965 | C ₄₇ H ₇₃ NO ₁₇ | 924.1 g/mol |  |
| 5. | Cinnamaldehyde | 637511 | C ₉ H ₈ O | 132.16 g/mol |  |
| 6. | Citral | 638011 | C ₁₀ H ₁₆ O | 152.23 g/mol |  |
| 7. | Caspofungin | 2826718 | C ₅₂ H ₈₈ N ₁₀ O ₁₅ | 1093.3 g/mol |  |
| 8. | Micafungin | 477468 | C ₅₆ H ₇₁ N ₉ O ₂₃ S | 1270.3 g/mol |  |

Table 1C. Type-III drugs used for *in silico* study against virulent proteins of SARS-CoV-2 (cont.).

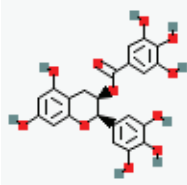
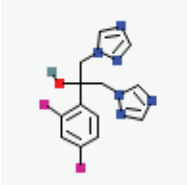
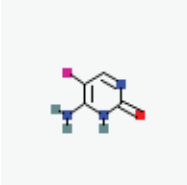
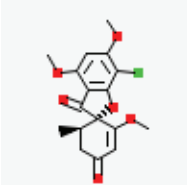

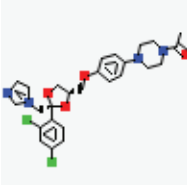
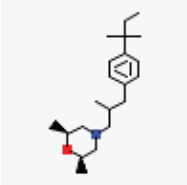
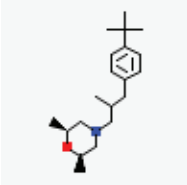
| S. N. | Compound | PubChem ID | Molecular formula | Molecular weight | 2D structure |
|-------|--------------------------|------------|--------------------------|------------------|---|
| 9. | Epigallocatechin gallate | 65064 | $C_{22}H_{18}O_{11}$ | 458.4 g/mol |  |
| 10. | Fluconazole | 3365 | $C_{13}H_{12}F_2N_6O$ | 306.27 g/mol |  |
| 11. | 5-Flucytosine | 3366 | $C_4H_4FN_3O$ | 129.09 g/mol |  |
| 12. | Griseofulvin | 441140 | $C_{17}H_{17}ClO_6$ | 352.8 g/mol |  |
| 13. | Itraconazole | 3793 | $C_{35}H_{38}Cl_2N_8O_4$ | 705.6 g/mol |  |
| 14. | Ketoconazole | 456201 | $C_{26}H_{28}Cl_2N_4O_4$ | 531.4 g/mol |  |
| 15. | Amorolfine | 49010 | $C_{21}H_{35}NO$ | 317.5 g/mol |  |
| 16. | Fenpropimorph | 93365 | $C_{20}H_{33}NO$ | 303.5 g/mol |  |

Table 1C. Type-III drugs used for *in silico* study against virulent proteins of SARS-CoV-2 (cont.).

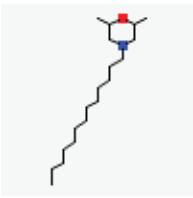




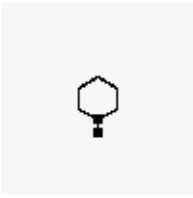

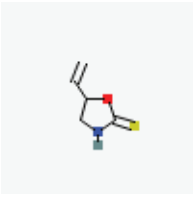
| S. N. | Compound | PubChem ID | Molecular formula | Molecular weight | 2D structure |
|-------|-------------------|------------|---|------------------|---|
| 17. | Tridemorph | 32518 | C ₁₉ H ₃₉ NO | 297.5 g/mol |  |
| 18. | α-Pinene | 6654 | C ₁₀ H ₁₆ | 136.23 g/mol |  |
| 19. | β-Pinene | 14896 | C ₁₀ H ₁₆ | 136.23 g/mol |  |
| 20. | 1-Aminopiperidine | 16658 | C ₅ H ₁₂ N ₂ | 100.16 g/mol |  |
| 21. | 4-Aminopiperidine | 424361 | C ₅ H ₁₂ N ₂ | 100.16 g/mol |  |
| 22. | Piperidine | 8082 | C ₅ H ₁₁ N | 85.15 g/mol |  |
| 23. | Dithiocarbamate | 3037131 | CH ₂ NS ₂ ⁻ | 92.17 g/mol |  |
| 24. | Goitrin | 3034683 | C ₅ H ₇ NOS | 129.18 g/mol |  |

Table 1C. Type-III drugs used for *in silico* study against virulent proteins of SARS-CoV-2 (cont.).

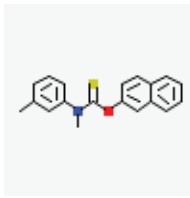
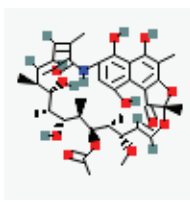
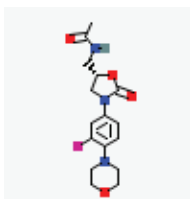
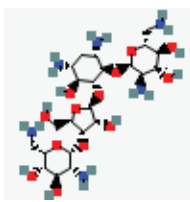
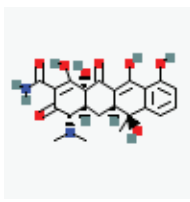
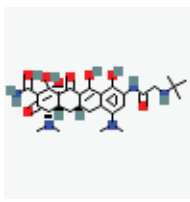
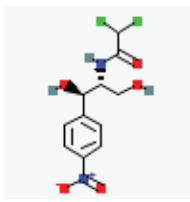

| S. N. | Compound | PubChem ID | Molecular formula | Molecular weight | 2D structure |
|-------|-----------------|------------|---|------------------|---|
| 25. | Tolnaftate | 5510 | C ₁₉ H ₁₇ NOS | 307.4 g/mol |  |
| 26. | Rifamycin | 6324616 | C ₃₇ H ₄₇ NO ₁₂ | 697.8 g/mol |  |
| 27. | Linezolid | 441401 | C ₁₆ H ₂₀ FN ₃ O ₄ | 337.35 g/mol |  |
| 28. | Neomycin | 8378 | C ₂₃ H ₄₆ N ₆ O ₁₃ | 614.6 g/mol |  |
| 29. | Tetracycline | 54675776 | C ₂₂ H ₂₄ N ₂ O ₈ | 444.4 g/mol |  |
| 30. | Tigecycline | 54686904 | C ₂₉ H ₃₉ N ₅ O ₈ | 585.6 g/mol |  |
| 31. | Chloramphenicol | 5959 | C ₁₁ H ₁₂ Cl ₂ N ₂ O ₅ | 323.13 g/mol |  |
| 32. | Quinupristin | 5388937 | C ₅₃ H ₆₇ N ₉ O ₁₀ S | 1022.2 g/mol |  |

Table 1C. Type-III drugs used for *in silico* study against virulent proteins of SARS-CoV-2 (cont.).

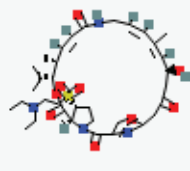
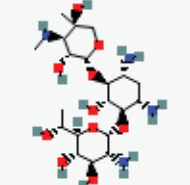
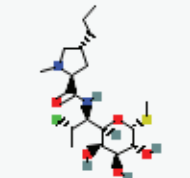
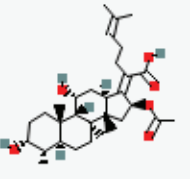

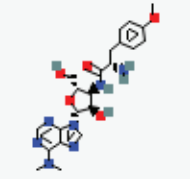

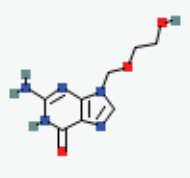
| S. N. | Compound | PubChem ID | Molecular formula | Molecular weight | 2D structure |
|-------|---------------|------------|----------------------------|------------------|---|
| 33. | Dalfopristin | 6323289 | $C_{34}H_{50}N_4O_9S$ | 690.8 g/mol |  |
| 34. | Geneticin | 123865 | $C_{20}H_{40}N_4O_{10}$ | 496.6 g/mol |  |
| 35. | Clindamycin | 446598 | $C_{18}H_{33}ClN_2O_5S$ | 425 g/mol |  |
| 36. | Fusidic acid | 3000226 | $C_{31}H_{48}O_6$ | 516.7 g/mol |  |
| 37. | Ricin | 9821402 | $C_{19}H_{36}O_3$ | 312.5 g/mol |  |
| 38. | Puromycin | 439530 | $C_{22}H_{29}N_7O_5$ | 471.5 g/mol |  |
| 39. | Virginiamycin | 127053480 | $C_{71}H_{84}N_{10}O_{17}$ | 1349.5 g/mol |  |
| 40. | Aciclovir | 135398513 | $C_8H_{11}N_5O_3$ | 225.2 g/mol |  |

Table 1C. Type-III drugs used for *in silico* study against virulent proteins of SARS-CoV-2 (cont.).

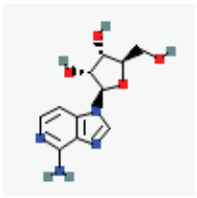
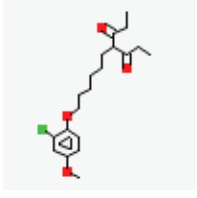
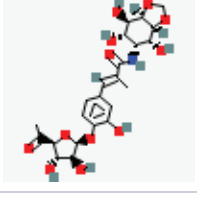
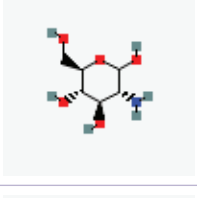
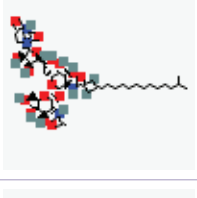
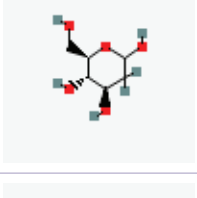
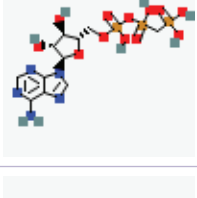
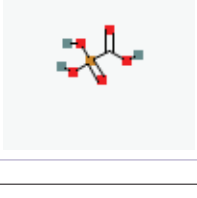
| S. N. | Compound | PubChem ID | Molecular formula | Molecular weight | 2D structure |
|-------|--|------------|---|------------------|---|
| 41. | 3-Deaza-adenosine | 23190 | C ₁₁ H ₁₄ N ₄ O ₄ | 266.25 g/mol |  |
| 42. | Arildone | 41782 | C ₂₀ H ₂₉ ClO ₄ | 368.9 g/mol |  |
| 43. | Hygromycin | 6433481 | C ₂₃ H ₂₉ NO ₁₂ | 511.5 g/mol |  |
| 44. | D-glucosamine | 439213 | C ₆ H ₁₃ NO ₅ | 179.17 g/mol |  |
| 45. | Tunicamycin | 11104835 | C ₄₀ H ₆₆ N ₄ O ₁₆ | 859 g/mol |  |
| 46. | 2-Deoxy-D-glucose-[1,2,3H(N)] | 91871895 | C ₆ H ₁₂ O ₅ | 170.18 g/mol |  |
| 47. | Adenosine-5'-[beta, gamma-methylene]triphosphate | 46936826 | C ₁₁ H ₁₅ N ₅ Na ₃ O ₁₃ P ₃ | 587.15 g/mol |  |
| 48. | Foscarnet | 3415 | CH ₃ O ₅ P | 26.01 g/mol |  |

Table 1C. Type-III drugs used for *in silico* study against virulent proteins of SARS-CoV-2 (cont.).

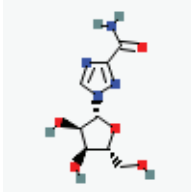
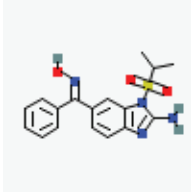
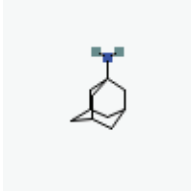
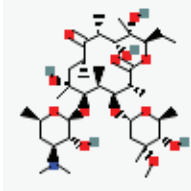
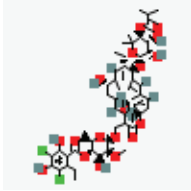
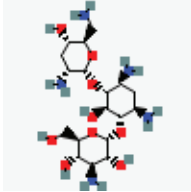
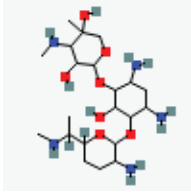
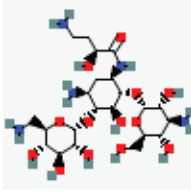
| S. N. | Compound | PubChem ID | Molecular formula | Molecular weight | 2D structure |
|-------|--------------|------------|---|------------------|---|
| 49. | Ribavirin | 37542 | C ₈ H ₁₂ N ₄ O ₅ | 244.2 g/mol |  |
| 50. | Enviroxime | 5361910 | C ₁₇ H ₁₈ N ₄ O ₃ S | 358.4 g/mol |  |
| 51. | Amantadine | 2130 | C ₁₀ H ₁₇ N | 151.25 g/mol |  |
| 52. | Erythromycin | 12560 | C ₃₇ H ₆₇ NO ₁₃ | 733.9 g/mol |  |
| 53. | Fidaxomicin | 10034073 | C ₅₂ H ₇₄ Cl ₂ O ₁₈ | 1058 g/mol |  |
| 54. | Tobramycin | 36294 | C ₁₈ H ₃₇ N ₅ O ₉ | 467.5 g/mol |  |
| 55. | Gentamicin | 25200338 | C ₂₁ H ₄₃ N ₅ O ₇ | 477.6 g/mol |  |
| 56. | Amikacin | 37768 | C ₂₂ H ₄₃ N ₅ O ₁₃ | 585.6 g/mol |  |

Table 2. Physicochemical and functional characterization of SARS-CoV-2 proteins.

| S. N. | Protein | PDB ID | Sequence length | Resolution | MW of protein | pI | Organism |
|-------|-----------|--------|-----------------|-------------|---------------|------|---------------------------|
| 1. | S protein | 6VXX | 1281 | 2.8 Å° | 141410.94 | 6.09 | SARS-CoV-2 |
| 2. | E protein | 5X29 | 81 | Through NMR | 8993.57 | 8.20 | SARS related corona virus |
| 3. | N protein | 6M3M | 136 | 2.7 Å° | 14876.63 | 9.60 | SARS-CoV-2 |
| 4. | nsp3 | 6W6Y | 170 | 1.45 Å° | 18254.81 | 6.31 | SARS-CoV-2 |
| 5. | nsp5 | 6M03 | 306 | 2.0 Å° | 33796.64 | 5.95 | SARS-CoV-2 |
| 6. | nsp10 | 2G9T | 152 | 2.10 Å° | 16125.36 | 5.84 | SARS related corona virus |
| 7. | nsp16 | 6W61 | 299 | 1 Å° | 33454.51 | 7.61 | SARS-CoV-2 |

CoV: Coronavirus; MW: Molecular weight; NMR: Nuclear magnetic resonance; pI: Isoelectric point.

Table 3. Protein validation and homology modeling estimation using the SWISS MODEL workspace.

| Protein | Template | Sequence identity (%) | Residues in favorable region (%) | Residues in unfavorable region (%) | C-β deviation | Q-mean score | Mol probity score |
|-----------|-----------|-----------------------|----------------------------------|------------------------------------|---|--------------|-------------------|
| S protein | 6zgh.1.C | 99.68 | 88.06 | 2.06 | 49 (A500-ASN, A410-CYS, A497-THR, A517-GLN, B131-SER, A404-THR, A360-VAL, A131-SER, A525-GLN, B39-THR, A427-ARG, A371-ALA, C497-THR, C234-ASP and A687-THR) | -3.32 | 1.65 |
| E protein | 2 mm4.1.A | 100 | 94.64 | 0 | - | -3.39 | 1.55 |
| N protein | 6y13.1.A | 100 | 96.90 | 0.78 | 2 (A11-THR and A65-ASP) | -0.21 | 1.32 |
| nsp3 | 6ywk.1.A | 100 | 99.40 | 0 | 0 | -0.04 | 0.50 |
| nsp5 | 6y2g.1.B | 100 | 97.67 | 0.17 | 7 (B221-ASN, A113-SER, A154-TYR, B33-ASP, A221-ASN, B282-LEU and B154-TYR) | -0.45 | 1.05 |
| nsp10 | 5c8s.1.A | 100 | 97.67 | 0 | - | -2.63 | 1.68 |
| nsp16 | 6w61.1.A | 100 | 97.98 | 0 | A98-ASP | -1.34 | 0.93 |

Table 4A. Docking energies (kcal/mol) of interaction between type-I drugs and SARS-CoV-2 target proteins.

| S. N. | Proteins | S-protein | E-protein | N-protein | nsp3 | nsp5 | nsp10 | nsp16 |
|-------|--------------------|-----------|-----------|-----------|----------|----------|----------|----------|
| | Ligands | | | | | | | |
| 1. | Baloxavir marboxil | -228.062 | -364.51 | -444.402 | -301.679 | -384.063 | -378.091 | -297.187 |
| 2. | Baricitinib | -148.24 | -236.938 | -288.915 | -196.09 | -249.641 | -245.762 | -193.172 |
| 3. | Chloroquine | -125.43 | -200.482 | -244.435 | -165.922 | -211.221 | -207.939 | -163.456 |
| 4. | Cobicistat | -189.883 | -226.358 | -257.405 | -221.819 | -255.857 | -285.876 | -246.005 |
| 5. | Danoprevir | -290.779 | -436.588 | -563.817 | -384.631 | -489.672 | -482.081 | -378.918 |
| 6. | Darunavir | -216.659 | -325.275 | -420.101 | -286.591 | -364.859 | -359.199 | -282.33 |
| 7. | Emtricitabine | -249.332 | -277.974 | -246.127 | -300.418 | -351.276 | -293.895 | -275.723 |
| 8. | Favipiravir | -62.717 | -93.4829 | -122.229 | -82.9615 | -105.612 | -103.973 | -81.7278 |
| 9. | Hydroxychloroquine | -109.732 | -99.3022 | -95.1757 | -98.7932 | -121.876 | -98.004 | -97.6645 |
| 10. | Lopinavir | -200.124 | -197.277 | -229.527 | -282.63 | -186.935 | -205.436 | -164.441 |
| 11. | Remdesivir | -239.465 | -359.523 | -466.708 | -316.756 | -403.267 | -397.008 | -312.051 |
| 12. | Ribavirin | -96.9263 | -154.915 | -188.877 | -128.218 | -163.221 | -160.683 | -126.307 |
| 13. | Ritonavir | -211.267 | -220.697 | -213.32 | -291.495 | -210.251 | -216.775 | -244.912 |
| 14. | Sofosbuvir | -205.256 | -308.184 | -397.956 | -271.515 | -345.646 | -340.27 | -267.473 |
| 15. | Tenofovir | -114.031 | -182.209 | -222.242 | -150.836 | -192.031 | -189.05 | -148.594 |
| 16. | Umifenovir | -140.352 | -153.644 | -93.3387 | -187.772 | -108.073 | -122.151 | -158.747 |

Table 4B. Docking energies (kcal/mol) of interaction between type-II drugs and SARS-CoV-2 target proteins.

| S. N. | Proteins | S-protein | E-protein | N-protein | nsp3 | nsp5 | nsp10 | nsp16 |
|-------|-----------------------|-----------|-----------|-----------|---------|---------|---------|---------|
| | Ligands | | | | | | | |
| 1. | Enalapril | -153.94 | -246.04 | -2010.23 | -203.63 | -259.24 | -255.21 | -200.6 |
| 2. | Captopril | -79.82 | -127.58 | -135.25 | -105.58 | -134.42 | -132.33 | -104.02 |
| 3. | Lisinolapril | -126.02 | -155.07 | -164.01 | -176.86 | -268.84 | -264.67 | -137.51 |
| 4. | Benzapril | -176.75 | -282.49 | -264.06 | -233.8 | -297.64 | -293.02 | -230.32 |
| 5. | Trandolpril | -176.75 | -282.5 | -248.68 | -233.8 | -297.64 | -293.03 | -230.32 |
| 6. | Perindopril | -148.24 | -236.94 | -214.26 | -196.1 | -249.64 | -245.76 | -193.17 |
| 7. | Fosinopril | -123.55 | -250.8 | -254.58 | -160.52 | -384.06 | -378.1 | -143.15 |
| 8. | Ramipril | -171.05 | -273.31 | -267.34 | -226.26 | -288.05 | -283.56 | -222.89 |
| 9. | Moexipril | -148.16 | -174.09 | -267.01 | -201.47 | -345.65 | -340.29 | -141.77 |
| 10. | Quinapril | -182.45 | -291.62 | -353.767 | -241.35 | -307.25 | -302.47 | -237.75 |
| 11. | Losartan | -158.17 | -122.45 | -175.26 | -125.6 | -297.65 | -293.03 | -110.49 |
| 12. | Irbesartan | -182.45 | -291.61 | -265.26 | -241.34 | -307.26 | -302.48 | -237.75 |
| 13. | Valsartan | -182.45 | -291.61 | -248.24 | -241.34 | -307.23 | -302.48 | -237.75 |
| 14. | Candesartan | -154.76 | -282.47 | -268.13 | -128.75 | -316.84 | -132.36 | -142.81 |
| 15. | Olmesartan | -146.59 | -108.17 | -215.03 | -145.4 | -316.84 | -168.24 | -108.74 |
| 16. | Telmisartan | -139.6 | -171.41 | -198.94 | -261.73 | -374.45 | -368.65 | -167.39 |
| 17. | Azilsartan | -193.85 | -291.06 | -298.28 | -256.43 | -326.45 | -321.38 | -252.61 |
| 18. | Hydrochlorothiazide | -79.63 | -70.81 | -84.04 | -103.21 | -163.22 | -88.82 | -81.7 |
| 19. | Chlorthalidone | -91.75 | -91.59 | -125 | -97.87 | -211.23 | -101.23 | -95.27 |
| 20. | Metolazone | -136.84 | -218.7 | -215 | -181 | -230.43 | -226.85 | -178.31 |
| 21. | Furosemide | -119.73 | -191.36 | -168 | -158.38 | -201.64 | -198.49 | -156.02 |
| 22. | Bumetanide | -84.44 | -114.14 | -147 | -112.85 | -240.05 | -106.56 | -167.75 |
| 23. | Amlodipine | -159.64 | -255.16 | -215.35 | -211.18 | -268.85 | -264.67 | -208.03 |
| 24. | Clevidipine | -171.05 | -256.8 | -235.15 | -226.26 | -288.04 | -283.58 | -222.89 |
| 25. | Diltiazem | -165.34 | -264.26 | -243.06 | -218.71 | -278.46 | -274.12 | -215.46 |
| 26. | Felodipine | -142.54 | -227.81 | -214.27 | -188.55 | -240.05 | -236.31 | -185.74 |
| 27. | Nisoldipine | -159.64 | -255.14 | -200.49 | -211.18 | -268.82 | -264.67 | -208.03 |
| 28. | Verapamil | -140.41 | -227.94 | -216.34 | -213.61 | -316.85 | -311.94 | -116.08 |
| 29. | Nebivolol | -133.55 | -177.04 | -187.14 | -135.84 | -278.44 | -111.75 | -140.87 |
| 30. | Carvedilol | -108.64 | -132.91 | -143.25 | -148.49 | -288.04 | -213.22 | -163.31 |
| 31. | Nadolol | -125.43 | -200.49 | -172.01 | -165.92 | -211.23 | -107.49 | -163.45 |
| 32. | Propranolol | -100.7 | -114.75 | -101.34 | -124.13 | -182.43 | -72.94 | -85.97 |
| 33. | Bisoprolol | -131.14 | -209.58 | -231.16 | -173.47 | -220.83 | -217.39 | -170.88 |
| 34. | Doxazosin | -139.58 | -131.05 | -214.64 | -172.02 | -316.85 | -221.87 | -228.57 |
| 35. | Terazosin | -159.64 | -255.19 | -220.94 | -211.18 | -268.83 | -128.03 | -208.03 |
| 36. | Hydralazine | -68.42 | -109.36 | -94.11 | -90.5 | -115.22 | -113.43 | -89.16 |
| 37. | Minoxidil | -85.52 | -136.69 | -124.26 | -113.13 | -144.03 | -141.78 | -111.45 |
| 38. | Atorvastatin | -156.53 | -228.89 | -215.45 | -205.56 | -393.66 | -220.28 | -225.69 |
| 39. | Fluvastatin | -156.57 | -105.86 | -135.15 | -155.94 | -288.05 | -188.96 | -120.96 |
| 40. | Parvastatin | -171.05 | -273.39 | -278.11 | -226.26 | -288.06 | -28356 | -222.89 |
| 41. | Aspirin | -74.12 | -111.82 | -112.68 | -98.05 | -124.82 | -122.8 | -96.59 |
| 42. | Clopidogrel bisulfate | -109.53 | -157.4 | -235.41 | -115.93 | -249.65 | -127.9 | -100.4 |
| 43. | Warfarin | -131.14 | -209.59 | -265.36 | -173.47 | -220.84 | -217.4 | -170.88 |
| 44. | Amiodarone | -142.28 | -161.05 | -248.11 | -156.1 | -297.64 | -131.8 | -225.57 |
| 45. | Flecainide | -159.64 | -239.7 | -215.01 | -211.17 | -268.85 | -264.67 | -208.03 |
| 46. | Procainamide | -96.93 | -154.92 | -188.27 | -128.21 | -163.21 | -160.69 | -126.3 |
| 47. | Sotalol | -102.63 | -164.03 | -154.15 | -135.75 | -172.83 | -170.14 | -133.73 |

Table 4B. Docking energies (kcal/mol) of interaction between type-II drugs and SARS-CoV-2 target proteins (cont.).

| S. N. | Proteins | S-protein | E-protein | N-protein | nsp3 | nsp5 | nsp10 | nsp16 |
|-------|------------------|-----------|-----------|-----------|---------|---------|---------|---------|
| | Ligands | | | | | | | |
| 48. | Digoxin | -242.81 | -212.72 | -265.15 | -314.06 | -528.11 | -320.66 | -339.47 |
| 49. | Amoxicillin | -142.54 | -227.82 | -254.39 | -188.55 | -240.04 | -236.29 | -185.75 |
| 50. | Doxycycline | -188.15 | -300.71 | -325.87 | -248.89 | -316.85 | -311.94 | -245.18 |
| 51. | Augmentin | -228.06 | -342.41 | -254.91 | -301.68 | -384.05 | -377.99 | -297.19 |
| 52. | Cephalexin | -136.84 | -218.71 | -264.01 | -181.01 | -230.44 | -226.85 | -178.31 |
| 53. | Azithromycin | -242.15 | -263.78 | -258.05 | -294.58 | -499.3 | -308.51 | -206.34 |
| 54. | Clarithromycin | -240.66 | -184.79 | -190.06 | -261.64 | -499.26 | -255.59 | -212.68 |
| 55. | Cefuroxime | -165.34 | -264.27 | -224.11 | -218.72 | -278 | -274.12 | -215.46 |
| 56. | Cefixime | -171.05 | -273.39 | -225.54 | -226.26 | -288.06 | -283.57 | -222.89 |
| 57. | Sulfamethoxazole | -216.66 | -346.29 | -301.19 | -286.6 | -364.86 | -359.19 | -282.33 |
| 58. | Dicloxacillin | -171.05 | -273.38 | -294.66 | -226.26 | -288.05 | -283.58 | -222.89 |

glycosylations of ACE-2 receptors in the host, which blocks binding of SARS-CoV-2 with the altered ACE-2. The *in silico*, *in vitro* and human trials, have proposed the immunomodulatory effect of chloroquine and its derivative hydroxychloroquine in critically ill SARS-CoV-2 infected patients and have indicated their promising role as effective antiviral drugs for the treatment of COVID-19 infections [38,39]. Apart from the aforementioned antiviral drugs, baloxavir marboxil, danoprevir, darunavir and sofosbuvir showed significant interaction with the main protease with the least binding energies, which are -384.06, -489.67, -364.859 and -345.646 kcal/mol, respectively.

Recent *in vitro* studies have demonstrated the role of darunavir in inhibition of viral entry and replication of SARS-CoV-2 via targeting viral protease [26]. However clinical trials for the safety and efficacy of darunavir are still undergoing [40].

The previous *in silico* study has identified RNA-dependent RNA polymerase as the target of sofosbuvir, which is a known antiviral drug used against RNA viruses. In clinical trials, the susceptibility of SARS-CoV-2 to sofosbuvir has been also explored [41]. The clinical efficacy of anti-influenza drugs like baloxavir marboxil and favipiravir was tested *in vitro* against SARS-CoV-2 and has been demonstrated to exhibit inhibitory potential against RNA synthesis [42].

Therefore, based on the previous *in silico*, *in vitro* and clinical studies as well as the present molecular docking analysis, it can be suggested that besides remdesivir, chloroquine and hydroxychloroquine; other antivirals like baloxavir marboxil, danoprevir and sofosbuvir represent an alternative and a novel drug candidate against SARS-CoV-2. However, drug likeliness report in our investigation also depicted that danoprevir, darunavir, favipiravir and lopinavir are toxic as they have violated three to four rules from Lipinski's rule of five. The toxicity level of danoprevir could restrict its application as a potent candidate for antiviral therapy; however, the dose regime of the drug is one of the highlighted parameters which is important to be analyzed for the drug toxicity [43].

SARS-CoV-2 enters the host cell by binding to its surface receptors called ACE-2, which are expressed by alveolar epithelial cells [22]. ACE-2 is closely related to ACE, a target of hypertensive drugs. ACE converts angiotensin-I to angiotensin-II, which is known for the narrowing of blood vessels and an increase in blood pressure. Angiotensin-II binds to the target ACE-2 receptors, releasing vasodilatation (angiotensin 1-7). Recent studies have demonstrated the downregulation of ACE-2 in response to viral attachment and deteriorating the health conditions of patients with comorbid conditions like hypertension and RTIs [43,44].

The antihypertensive drugs block angiotensin-I-mediated vasoconstriction and enhance the expression of ACE-2 on the cell surface. This mechanism might impart protection to the lungs and prevents the patients from the high risk associated with SARS-CoV-2 [45,46]. We have investigated the interaction of 58 drugs under the type-II category including ACE-2 inhibitors, ARBs, α - and β -blockers, anticoagulants, and RTI drugs. We identified seven drugs including fosinopril, moexipril, quinapril, telmisartan, azilsartan, verapamil and doxazosin to possess significant interaction with the main protease of SARS-CoV-2. The ACE-2 inhibitors like fosinopril, moexipril and quinapril

Table 4C. Docking energies (kcal/mol) of interaction between type-III drugs and SARS-CoV-2 target proteins.

| S. N. | Proteins ↓ Ligands | S-protein | E-protein | N-protein | nsp3 | nsp5 | nsp10 | nsp16 |
|-------|-------------------------------|-----------|-----------|-----------|---------|---------|---------|----------|
| 1. | 1-Amino piperidine | -40.60 | -58.77 | -75.37 | -53.28 | -68.25 | -71.43 | -52.79 |
| 2. | 4- Amino piperidine | -45.35 | -71.00 | -78.06 | -56.35 | -72.62 | -74.51 | -53.82 |
| 3. | α-Pinene | -38.13 | -43.60 | -60.47 | -54.18 | -31.95 | -99.42 | -27.10 |
| 4. | Amorolfine | -103.42 | -124.62 | -77.7 | -108.96 | -218.57 | -72.27 | -99.91 |
| 5. | Amphotericine B | -301.25 | -391.72 | -702.11 | -412.79 | -245.04 | -386 | -267.52 |
| 6. | β-Pinene | -57.01 | -91.13 | -111.12 | -75.42 | -96.01 | -99.45 | -74.29 |
| 7. | Butenafine hydrochloride | -97.92 | -106.02 | -113.11 | -124.31 | -119.76 | -118.72 | -108.14 |
| 8. | Caspofungin | -298.74 | -427.92 | - 327 | -292.2 | -298 | -325 | -330.38 |
| 9. | Cinnamaldehyde | -56.40 | -90.66 | -108.91 | -75.72 | -95.35 | -98.72 | -72.67 |
| 10. | Citral | -45.23 | -33.28 | -63.39 | -47.74 | -23.66 | -55.48 | -51.06 |
| 11. | Dithiocarbamate | -25.08 | -39.67 | -44.28 | -31.64 | -41.08 | -42.16 | -30.35 |
| 12. | Epigallocatechin gallate | -83.40 | -174.39 | -17.25 | -161.28 | -118.68 | -152.2 | -191.814 |
| 13. | Fenpropimorph | -123.89 | -199.54 | -240.04 | -165.78 | -209.04 | -216.6 | -160.21 |
| 14. | Fluconazole | -131.84 | -202.21 | -239.46 | -171.23 | -217.09 | -221.59 | -169.27 |
| 15. | 5-Flucytosine | -61.33 | -92.48 | -101.51 | -75.28 | -93.09 | -98.67 | -73.99 |
| 16. | Goitrin | -41.77 | -72.904 | -85.38 | -61.03 | -77.82 | -80 | -59.19 |
| 17. | Griseofulvin | -122.64 | -119.80 | -56.18 | -139.75 | -93.51 | -244.47 | -116.51 |
| 18. | Itraconazole | -153.29 | -157.55 | -523.02 | -263.99 | -463.65 | -96 | -175.02 |
| 19. | Ketoconazole | -278.61 | -412.63 | -522.99 | -368.66 | -463.78 | -125 | -369.65 |
| 20. | Micafungin | -424.67 | -771.03 | -694 | -473.01 | -684 | -115 | -375.32 |
| 21. | Naftifine | -124.66 | -187.79 | -240.88 | -164.75 | -209.25 | -213.6 | -161.82 |
| 22. | Piperidine | -34.96 | -55.19 | -64.94 | -15.55 | -60.2 | -61.34 | -44.98 |
| 23. | Terbinafine | -98.843 | -111.47 | -66.61 | -104.72 | -209.26 | -88.67 | -89.11 |
| 24. | Tolnaftate | -123.89 | -199.54 | -238.58 | -165.79 | -209.07 | -216.21 | -160.2 |
| 25. | Tridemorph | -118.19 | -190.44 | -228.94 | -158.32 | -199.58 | -204.27 | -152.77 |
| 26. | Rifamycin | -171.17 | -311.64 | -301.14 | -273.4 | -480.06 | -472.63 | -310.03 |
| 27. | Linezolid | -136.84 | -218.7 | -185.10 | -181 | -230.44 | -226.85 | -178.31 |
| 28. | Neomycin | -191.68 | -229.63 | -264.02 | -261.63 | -403.26 | -220.78 | -114.4 |
| 29. | Tetracycline | -151.37 | -188.99 | -116.57 | -164.82 | -307.25 | -198.74 | -152.57 |
| 30. | Tigecycline | -218.25 | -278.52 | -198.06 | -178.26 | -403.22 | -351.05 | -172.87 |
| 31. | Chloramphenicol | -114.03 | -182.26 | -146.11 | -150.84 | -192.04 | -189.04 | -148.59 |
| 32. | Quinupristin | -297.34 | -311.92 | -336.379 | -368.05 | -700.91 | -380.32 | -281.08 |
| 33. | Dalfopristin | -246.47 | -277.18 | -265.68 | -338.37 | -460.89 | -312.77 | -214.5 |
| 34. | Geneticin | -193.85 | -309.83 | -249.33 | -256.43 | -326.45 | -321.38 | -252.61 |
| 35. | Clindamycin | -153.94 | -246.03 | -201.48 | -203.64 | -259.25 | -255.22 | -200.6 |
| 36. | Fusidic Acid | -192.46 | -240.61 | -185.24 | -214.79 | -355.25 | -148.98 | -168.46 |
| 37. | Ricin | -134.93 | -135.16 | -157.11 | -163.59 | -268.85 | -165.92 | -171.91 |
| 38. | Puromycin | -151.35 | -149.37 | -231.92 | -143.21 | -326.45 | -216.18 | -156.53 |
| 39. | Virginiamycin | -428.28 | -399.22 | -624.25 | -589.65 | -940.99 | -453.95 | -479.18 |
| 40. | Aciclovir | -91.22 | -69.48 | -116.94 | -120.67 | -153.63 | -81 | -118.88 |
| 41. | 3-deaza-adenosine | -56.34 | -87.07 | -115.45 | -97.44 | -182.43 | -94.41 | -77.39 |
| 42. | Arildone | -142.54 | -227.81 | -192.19 | -188.54 | -240.04 | -236.31 | -185.75 |
| 43. | Hygromycin | -147.28 | -201.78 | -168.02 | -185.82 | -345.65 | -229.91 | -133.34 |
| 44. | D-glucosamine | -68.42 | -109.35 | -92.55 | -90.5 | -115.22 | -113.43 | -89.16 |
| 45. | Tunicamycin | -222.77 | -239.28 | -385.75 | -265.18 | -556.88 | -491.97 | -254.01 |
| 46. | 2-Deoxy-D-glucose-[1,2,3H(N)] | -62.72 | -100.24 | -89.36 | -82.96 | -105.61 | -103.98 | -81.73 |

Table 4C. Docking energies (kcal/mol) of interaction between type-III drugs and SARS-CoV-2 target proteins (cont.).

| S. N. | Proteins | S-protein | E-protein | N-protein | nsp3 | nsp5 | nsp10 | nsp16 |
|-------|---|-----------|-----------|-----------|---------|---------|---------|---------|
| | Ligands | | | | | | | |
| 47. | Adenosine-5'-(beta, gamma-methylene)triphosphate] | -124.9 | -157.22 | -216.14 | -133.41 | -297.66 | -241.35 | -132.92 |
| 48. | Foscarnet | -39.91 | -59.92 | -53.39 | -52.79 | -67.21 | -66.17 | -52.01 |
| 49. | Ribavirin | -96.93 | -154.92 | -156.59 | -128.22 | -163.22 | -160.69 | -126.31 |
| 50. | Enviroxime | -142.54 | -227.81 | -214.33 | -188.55 | -240.03 | -236.31 | -185.75 |
| 51. | Amantadine | -62.72 | -100.23 | -87.15 | -82.96 | -105.62 | -103.97 | -81.73 |
| 52. | Erythromycin | -235.04 | -233.44 | -256.28 | -293.6 | -489.67 | -244.59 | -232.53 |
| 53. | Fidaxomicin | -338.94 | -321.37 | -450.38 | -376.44 | -691.29 | -646.51 | -460.32 |
| 54. | Tobramycin | -182.45 | -273.94 | -265.11 | -241.34 | -307.25 | -302.48 | -237.75 |
| 55. | Gentamicin | -176.75 | -282.5 | -268.36 | -233.8 | -297.65 | -293.03 | -230.32 |
| 56. | Amakicin | -174.13 | -178.01 | -230.39 | -187.86 | -384.06 | -221.29 | -183.59 |

demonstrated the most significant docking poses with the main protease and N protein with the lowest binding energy.

Furthermore, investigation of docking analysis of ARBs and molecular targets of SARS-CoV-2 showed effective binding affinity of telmisartan, azilsartan, verapamil and doxazosin toward main protease. Recent studies have also depicted the role of antihypertensives such as losartan, olmesartan and telmisartan as antiviral agents against SARS-CoV-2 infection while the clinical trial of telmisartan for COVID-19 therapy has recently started [47,48]. Henceforth, the role of these antihypertensive drugs as promising anti-SARS-CoV-2 drugs cannot be ruled out and could be a subject of future research for assessing their application as repurposed drugs in COVID-19 infection.

The structural and nonstructural viral proteins have the most gruesome role in its infection cycle. Considering their importance in viral attachment, invasion, replication and pathogenicity, we have studied the possible effect of antimicrobial agents targeting the protein or their synthesis. In our computational study, we investigated the binding affinity of 56 such miscellaneous drugs that interacted effectively with the binding site of SARS-CoV-2 proteins. There are previous experimental proofs that have highlighted the application and potential of various antibacterial and antifungal agents targeting intracellular processes like replication, protein synthesis, and cell cycle in viruses like vesicular stomatitis virus, herpes simplex virus types 1, Sindbis virus, influenza virus, vaccinia virus and HIV-1 [49–52].

Antibacterial drugs such as azithromycin, doxycycline, clarithromycin, rifamycin and augmentin (a combination of amoxicillin and clavulanate) are specifically used for the treatment of throat, chest infection and pneumonia. In our study, these antibiotics were identified to exhibit significant binding efficacy at the target site of the main protease (nsp-5) and nsp10. The antiviral potential of several other antibacterial drugs like lymecycline, demeclocycline and eravacycline has been studied *in silico* and *in vitro*, which also indicated the possible application of antibiotics drugs against SARS-CoV-2 [53]. The possible mechanism of the antiviral effect of these antibiotics could lie in the immunopathology of SARS-CoV-2 that resulted in decreased expression of CD-147, which is a transmembrane glycoprotein belonging to the immunoglobulin superfamily. The CD-147 glycoproteins are expressed by epithelial cells, macrophages and type II pneumocytes, and act as an upstream stimulator of matrix metalloproteinases and induce progression of cancer cells. Wang *et al.* have demonstrated CD-147 as an effective receptor SARS-CoV-2 S protein [53]. Antibiotics such as doxycycline and azithromycin have shown reduced expression of CD-147 on carcinoma cell lines, and therefore, these agents could prove to be a possible repurpose drug candidate for SARS-CoV-2 [54].

The present study showed that virginiamycin, tunicamycin, quinipristin, fidaxomicin, digoxin and azithromycin exhibited stable interaction to the residues in the binding pockets of the main protease with the least binding energies. In a previous study, fidaxomicin has also shown effective antiviral efficacy against other viruses like the ZIKA virus and has depicted inhibition of RNA-dependent RNA polymerase and subsequent viral infection *in vitro* and *in vivo* [55]. Antifungal drugs like caspofungin, amphotericin B, ketoconazole and macfungin were found to elicit antiviral effect by showing significant binding affinity toward E and N proteins. In different studies conducted

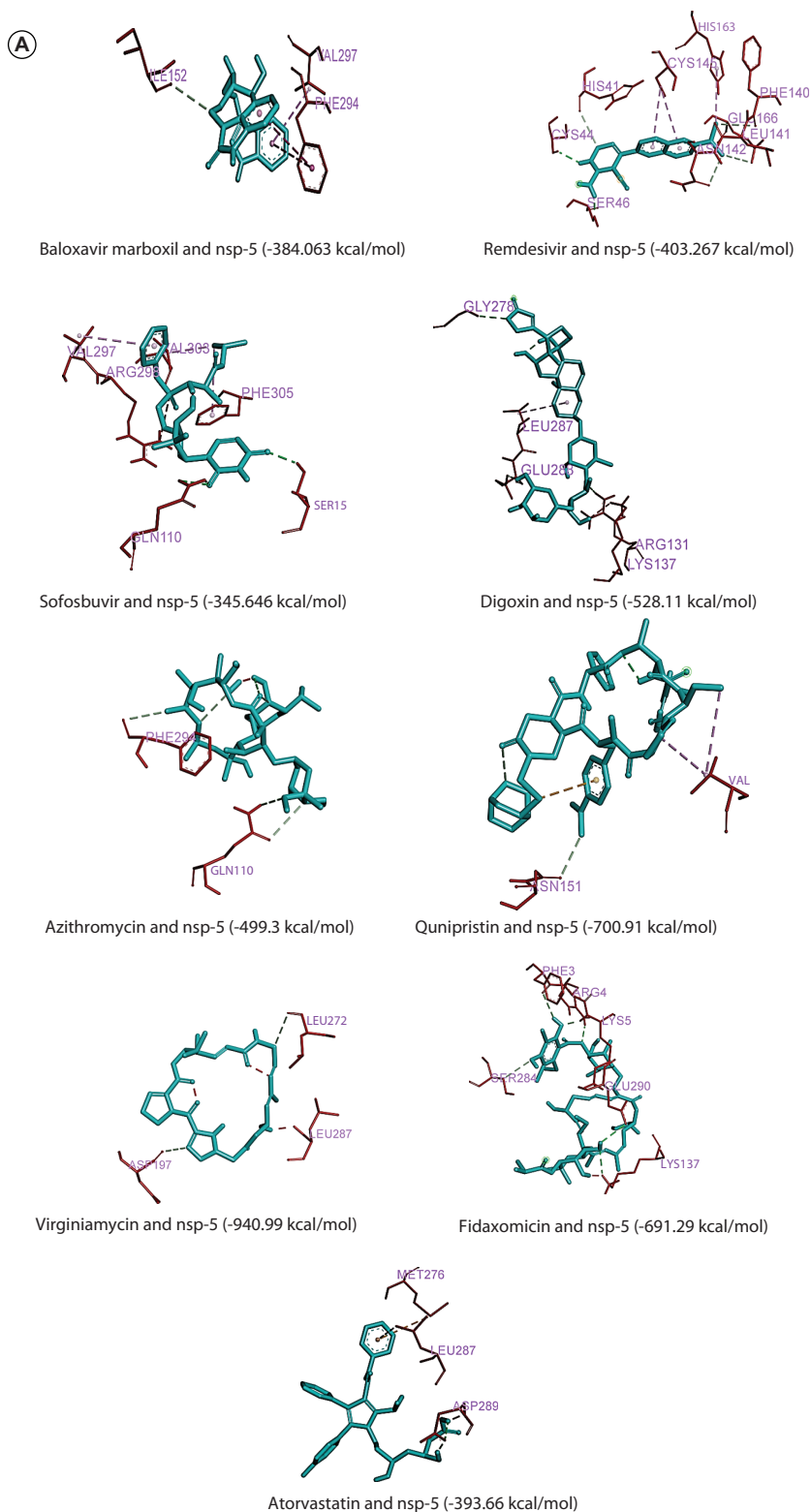


Figure 2. Molecular docking images of interaction between ligands and SARS-CoV-2 proteins. (A) Molecular docking images of most efficient interaction between ligands and SARS-CoV-2 nsp5 protein. **(B)** Molecular docking images of most efficient interaction between ligands and SARS-CoV-2 nsp10 protein. **(C)** Molecular docking images of most efficient interaction between ligands and SARS-CoV-2 N-protein. **(D)** Molecular docking images of most efficient interaction between ligands and SARS-CoV-2 E-protein. CoV: Coronavirus.

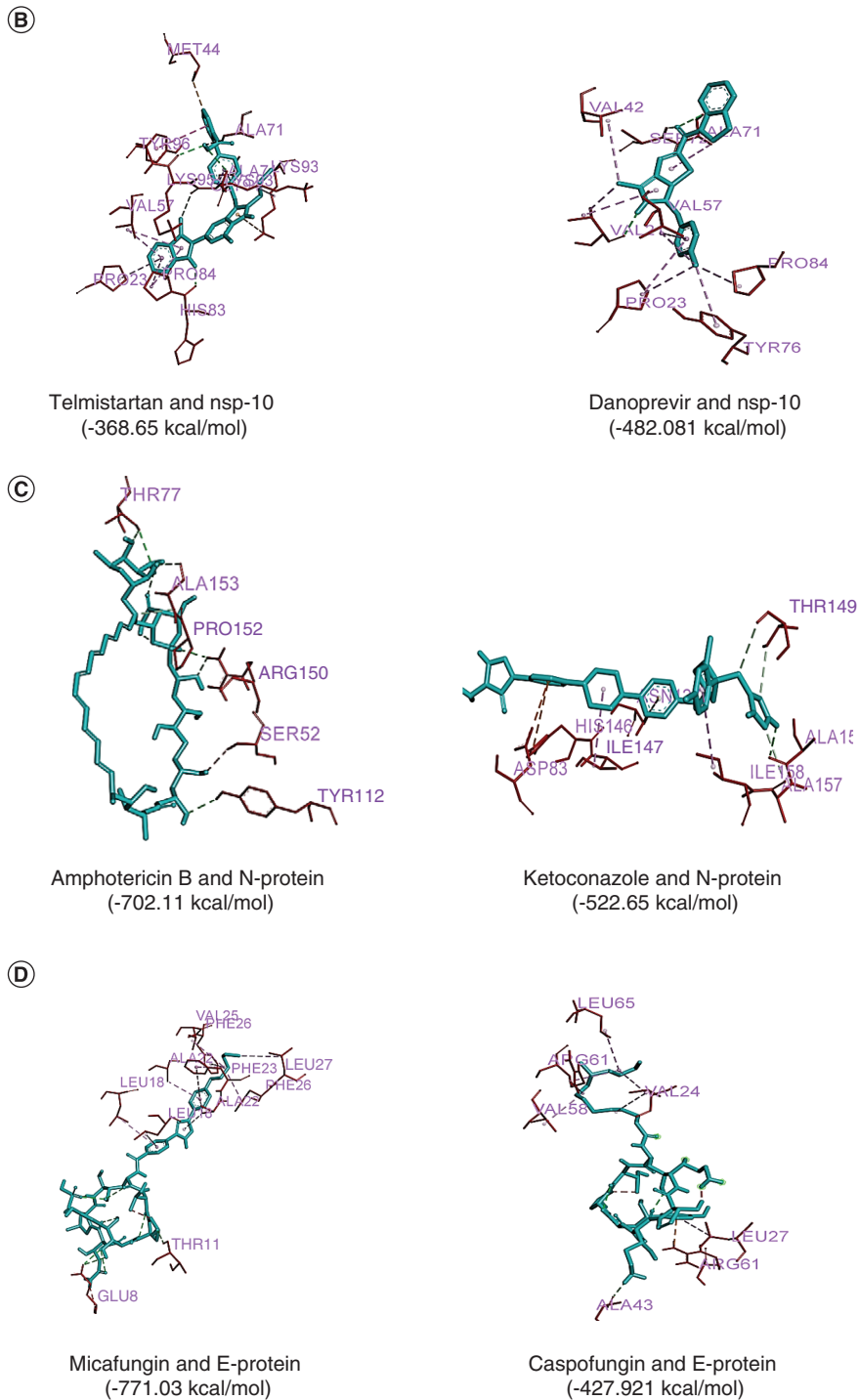


Figure 2. Molecular docking images of interaction between ligands and SARS-CoV-2 proteins (cont.). (A) Molecular docking images of most efficient interaction between ligands and SARS-CoV-2 nsp5 protein. **(B)** Molecular docking images of most efficient interaction between ligands and SARS-CoV-2 nsp10 protein. **(C)** Molecular docking images of most efficient interaction between ligands and SARS-CoV-2 N-protein. **(D)** Molecular docking images of most efficient interaction between ligands and SARS-CoV-2 E-protein. CoV: Coronavirus.

against enterovirus 71, the inhibitory potentials of antifungal drugs like micafungin and amphotericin B were mentioned against enterovirus 71 [50,51].

The spike glycoprotein (S protein) plays an essential role in the wide host tropism of SARS-COV-2 and mediates its pathogenicity via binding to host cell surface receptors and enabling its entry into the host cell [40,41]. Out of 130 drugs, two of the antibiotics namely virginiamycin (-428.28 kcal/mol) and amphotericin B (-301.254 kcal/mol) revealed strong interaction with S protein in the present molecular docking study. Therefore, it is a matter of future investigation to assess whether these antibiotics could prevent cleavage and activation of S1/S2 subunits of S protein and hence could inhibit viral attachment to the host cell receptor.

Mammalian metabolism and toxicity of all the proposed repurposed drugs were tested through ADMET analysis using SWISS-ADME server and admetSAR version 2.0. In terms of drug development; solubility, dissolution and permeability across the GI barrier are the prime focus since drug absorption is important before any associated medical effect can be induced. The solubility and the GI absorption are essential and rate-limiting steps for preformulation interpretations in drug development [56,57]. The potency of any drug is also determined by its ability to reach the blood–brain barrier, which isolates brain tissues from the substances circulating in the blood vascular system. The present study indicated poor membrane permeation properties of all the tested 130 drugs across endothelial capillaries (blood–brain barrier) [58,59].

Permeability glycoprotein (Pgp) or CD243 is an ATP-dependent drug efflux pump extensively distributed and expressed as a receptor on intestinal epithelium that pumps toxins or drugs back into the intestinal lumen and liver [60,61]. CYP450 (CYP3A4) is the main enzyme that catalyzes drug metabolism in the intestine and liver. The co-existence of CYP3A4 and Pgp at the same site synergistically reduces the bioavailability of the drug [62,63]. There was no overlapping observed in CYP3A4 and Pgp suggesting the high bioavailability of the tested drugs.

The study unveils the lipophilic property of all 130 drugs and showed the lipophilic nature of 122 drugs with a positive value of Log P (Log p > 0), while drugs like foscarnet, adenosine-5'-[beta, gamma-methylene] triphosphate, augmentin, minoxidil, hydrochlorothiazide, losartan and fosinopril indicated their hydrophilic nature and higher affinity for the aqueous phase (negative value of Log P). The optimization of pharmacodynamic and pharmacokinetic characteristics of hits and leads in drug development is crucial and is highly dependent on the drug lipophilicity [64,65].

Conclusion

In the current study, out of 130 drugs that belong to the different class, 15 drugs were identified to be the significant inhibitors of SARS-CoV-2 proteins. The computational study of the target protein and drugs molecular interaction highlighted the potential of baloxavir marboxil, danoprevir, sofosbuvir, fosinopril, quinapril, telmisartan, atrovastatin, sulfamethoxazole, clarithromycin, micafungin, virginiamycin, tunicamycin, fidaxomicin, amphotericin B and caspofungin as a potent inhibitor of SARS-CoV-2 proteins, and therefore, these identified compounds could be explored for their role as future drug candidates against COVID-19.

The biochemical characterization, the pharmacokinetics of the aforementioned potent drugs and the computational analysis of their molecular interactions with SARS-CoV-2 proteins have provided preliminary breakthrough which could lead to exploring their avenues in repurposed drug development. It is pertinent that drug repurposing is an alternative way to curb pandemics like medical emergencies and thus their efficacy to combat SARS-CoV-2 related serious health complications should be explored.

Hence, the effectiveness of baloxavir marboxil, danoprevir, sofosbuvir, fosinopril, quinapril, telmisartan, atrovastatin, sulfamethoxazole, clarithromycin, micafungin, virginiamycin, tunicamycin, fidaxomicin, amphotericin B and caspofungin targeting the structural and nonstructural proteins indicates the possibilities of success of repurposing these drugs against SARS-COV-2. Further *in vitro* and *in vivo* studies of screened compounds alone and their varying combinations could provide an insight into the development and application of these compounds as potent anti-SARS-CoV-2 drugs.

Future perspective

The study attempted to highlight the inhibitory potential of drugs namely, baloxavir marboxil, danoprevir, sofosbuvir, fosinopril, quinapril, telmisartan, atrovastatin, sulfamethoxazole, clarithromycin, micafungin, virginiamycin, tunicamycin, fidaxomicin, amphotericin B and caspofungin, and thus, revealed their prospects in drug repurposing to combat SARS-CoV-2. The study might lead the way for clinicians, pharmaceutical experts to investigate and further validate these compounds as potent novel and efficacious antiviral therapy against COVID-19 infection.

Summary points

- The study investigated the inhibitory potential and molecular targets of 130 compounds categorized into three types: antivirals (type-I); drugs used in cardiovascular diseases, respiratory tract infection and hypertension (type-II); and antibacterial/antifungal drugs (type-III) against SARS-CoV-2 through computational docking tools.
- Out of 130 compounds, 15 drugs were identified to be significant inhibitors of SARS-CoV-2 and showed a favorable binding affinity with viral S protein, N protein, E- protein, nsp-5, nsp10, nsp-16.
- The identified potent drug candidates such as baloxavir marboxil, danoprevir, sofosbuvir, fosinopril, quinapril, telmisartan, atorvastatin, sulfamethoxazole, clarithromycin, micafungin, virginiamycin, tunicamycin, fidaxomicin, amphotericin B and caspofungin showed promising pharmacokinetic properties and low acute toxicity profile.
- The investigation might lead the way for authenticating the inhibitory potential of these screened compounds by *in vitro* and *in vivo* studies, and further exploring their activity and applications as an individual compound or in varying combinations against SARS-CoV-2.

Supplementary data

To view the supplementary data that accompany this paper please visit the journal website at: www.futuremedicine.com/doi/suppl/10.2217/fvl-2020-0403

Author contributions

All the authors equally contributed in the study.

Acknowledgments

We are highly thankful to the Department of Biotechnology and Life Sciences, Graphic Era (Deemed to be University) for giving us the opportunity and providing all the technical facility to execute this extensive study.

Financial & competing interests disclosure

The authors have no relevant affiliations or financial involvement with any organization or entity with a financial interest in or financial conflict with the subject matter or materials discussed in the manuscript. This includes employment, consultancies, honoraria, stock ownership or options, expert testimony, grants or patents received or pending, or royalties.

No writing assistance was utilized in the production of this manuscript.

References

1. Du L, He Y, Zhou Y, Liu S, Zheng BJ, Jiang S. The spike protein of SARS-COV-2, a target for vaccine and therapeutic development. *Nat. Rev. Microbiol.* 7(3), 226–236 (2009).
2. Lai MM, Cavanagh D. The molecular biology of coronaviruses. *Adv. Virus Res.* 48, 1–100 (1997).
3. Zirkel F, Kurth A, Quan PL *et al.* An insect nidovirus emerging from a primary tropical rainforest. *mBio* 2(3), e00077–11 (2011).
4. De Groot RJ, Baker SC, Baric R *et al.* Middle East respiratory syndrome coronavirus (MERS-CoV): announcement of the coronavirus study group. *J. Virol.* 87(14), 7790–7792 (2013).
5. Khailany RA, Safdar M, Ozaslan M. Genomic characterization of a novel SARS-CoV-2. *Gene. Rep.* 19, 100682 (2020).
6. Susan RW, Sonia N. Coronavirus pathogenesis and the emerging pathogen severe acute respiratory syndrome coronavirus. *Microbiol. Mol. Biol. Rev.* 69(4), 635–664 (2005).
7. Gosert R, Kanjanahaluethai A, Egger D, Bienz K, Baker SC. RNA replication of mouse hepatitis virus takes place at double-membrane vesicles. *J. Virol.* 76(8), 3697–3708 (2002).
8. Mark RD. Seeking membranes: positive-strand RNA virus replication complexes. *PLoS Biol.* 6(10), e270 (2008).
9. Stertz S, Reichelt M, Spiegel M *et al.* The intracellular sites of early replication and budding of SARS-coronavirus. *Virology* 361(2), 304–315 (2007).
10. Ng ML, Tan SH, See EE, Ooi EE, Ling AE. Proliferative growth of SARS coronavirus in Vero E6 cells. *J. Gen. Virol.* 84(12), 3291–3303 (2003).
11. Tan YJ, Lim SG, Hong W. Characterization of viral proteins encoded by the SARS-coronavirus genome. *Antiviral Res.* 65(2), 69–78 (2005).
12. de Haan CA, Masters PS, Kuo L, Vennema H, Rottier Peter JM. Coronavirus particle assembly: primary structure requirements of the membrane protein. *J. Virol.* 72(8), 6838–6850 (1998).
13. Escors D, Ortego J, Laude H, Enjuanes L. The membrane M protein carboxy terminus binds to transmissible gastroenteritis coronavirus core and contributes to core stability. *J. Virol.* 75(3), 1312–1324 (2001).

14. Raamsman MJB, Locker JK, de Hooge A *et al.* Characterization of the coronavirus mouse hepatitis virus strain A59 small membrane protein E. *J. Virol.* 74(5), 2333–2342 (2000).
15. Baudoux P, Carrat C, Besnardeau L, Charley B, Laude H. Coronavirus pseudo particles formed with recombinant M and E proteins induce alpha interferon synthesis by leukocytes. *J. Virol.* 72(11), 8636–8643 (1998).
16. Dutta NK, Mazumdar K, Gordy JT. The nucleocapsid protein of SARS-CoV-2: a target for vaccine development. *J. Virol.* 94(13), e00647–20 (2020).
17. Xue X, Yu H, Yang H *et al.* Structures of two coronavirus main proteases: implications for substrate binding and antiviral drug design. *J. Virol.* 82(5), 2515–2527 (2008).
18. Xia B, Kang X. Activation and maturation of SARS-CoV main protease. *Prot. Cell.* 2(4), 282–290 (2011).
19. Zhang L, Lin D, Sun X *et al.* Crystal structure of SARS-CoV-2 main protease provides a basis for design of improved α -ketoamide inhibitors. *Science* 368(6489), 409–412 (2020).
20. Choudhury A, Mukherjee S. *In silico* studies on the comparative characterization of the interactions of SARS-CoV-2 spike glycoprotein with ACE-2 receptor homologs and human TLRs. *J. Med. Virol.* 92(10), 2105–2113 (2020).
21. Lai MM, Baric RS, Brayton PR, Stohlman SA. Studies on the mechanism of RNA synthesis of a murine coronavirus. In: *Molecular Biology and Pathogenesis of Coronaviruses*. Rottier PJM, van der Zeijst BAM, Spaan WJM, Horzinek MC (Eds). Advances in Experimental Medicine and Biology, vol. 173, Springer, MA, USA, 187–200 (1984).
22. Tikellis C, Thomas MC. Angiotensin-converting enzyme 2 (ACE2) is a key modulator of the renin angiotensin system in health and disease. *Int. J. Pept.* 2012, 8 (2012).
23. Nicin L, Abplanalp WT, Mellentin H *et al.* Cell type-specific expression of the putative SARS-CoV-2 receptor ACE2 in human hearts. *Eur. Heart J.* 41(19), 1804–1806 (2020).
24. Sanyaolu A, Okorie C, Marinkovic A *et al.* Comorbidity and its impact on patients with COVID-19. *SN Compr. Clin. Med.* 55(5), 1–8 (2020).
25. Dyll J, Coleman CM, Hart BJ *et al.* Repurposing of clinically developed drugs for treatment of Middle East respiratory syndrome coronavirus infection. *Antimicrob. Agents Chemother.* 58(8), 4885–4893 (2014).
26. Singh TU, Parida S, Lingaraju MC, Kesavan M, Kumar D, Singh RK. Drug repurposing approach to fight COVID-19. *Pharmacol. Rep.* 72(6), 1479–1508 (2020).
27. Zhou Y, Wang F, Tang J, Nussinov R, Cheng F. Artificial intelligence in COVID-19 drug repurposing. *Lancet Digit. Health* 2(12), e667–e676 (2020).
28. Mercorelli B, Palu G, Loregian A. Drug repurposing for viral infectious diseases: how far are we? *Trends Microbiol.* 26(10), 865–876 (2018).
29. Gasteiger E, Hoogland C, Gattiker A *et al.* Protein identification and analysis tools on the ExPASy server. In: *The Proteomics Protocols Handbook*. Walker JM (Ed.). Humana Press, NJ, USA, 571–607 (2005).
30. Arnold K, Bordoli L, Kopp J, Schwede T. The SWISS-MODEL workspace: a web-based environment for protein structure homology modeling. *Bioinformatics* 22(2), 195–201 (2006).
31. Waterhouse A, Bertoni M, Bienert S *et al.* SWISS-MODEL: homology modelling of protein structures and complexes. *Nucleic Acid Res.* 46(Suppl. 1), W296–W303 (2018).
32. Daina A, Michielin O, Zoete V. SwissADME: a free web tool to evaluate pharmacokinetics, drug-likeness and medicinal chemistry friendliness of small molecules. *Sci. Rep.* 7, 42717 (2017).
33. Daina A, Michielin O, Zoete V. iLOGP: a simple, robust, and efficient description of *n*-octanol/water partition coefficient for drug design using the GB/SA approach. *J. Chem. Inf. Model.* 54(12), 3284–3301 (2014).
34. Cheng F, Li W, Zhou Y *et al.* admetSAR: a comprehensive source and free tool for evaluating chemical ADMET properties. *J. Chem. Inf. Model.* 52(11), 3099–3105 (2020).
35. Kai-Cheng HC, Yen-Fu L, Shen-Rong Y, Jinn-Moon Y. iGEMDOCK: a graphical environment of enhancing GEMDOCK using pharmacological interactions and post-screening analysis. *BMC Bioinformatics* 12, S33 (2011).
36. Ray AK, Gupta PSS, Panda SK, Biswal S, Rana MR. Repurposing of FDA approved drugs for the identification of potential inhibitors of SARS-CoV-2 main protease. *ChemRxiv* (2020). Preprint. <https://doi.org/10.26434/chemrxiv.12278066.v2>
37. WHO R&D Blueprint. COVID-19: therapeutics working group consultation on the potential role of chloroquine in clinical management. (2020). www.who.int/publications/i/item/informal-consultation-on-the-potential-role-of-chloroquine-in-the-clinical-management-of-covid-19-infection
38. Yao X, Ye F, Zhang M *et al.* *In vitro* antiviral activity and projection of optimized dosing design of hydroxychloroquine for the treatment of severe acute respiratory syndrome coronavirus 2 (SARS-CoV-2). *Clin. Infect. Dis.* 71(15), 732–739 (2020).
39. Wang M, Cao R, Zhang L *et al.* Remdesivir and chloroquine effectively inhibit the recently emerged novel coronavirus (2019-nCoV) *in vitro*. *Cell. Res.* 30, 269–271 (2020).
40. Clinical trials.gov. Bethesda (MD): National Library of Medicine (US) – homepage. <https://ClinicalTrials.gov>.

41. Sayad B, Sobhani M, Khodarahm R. Sofosbuvir as repurposed antiviral drug against COVID-19: why were we convinced to evaluate the drug in a registered/approved clinical trial? *Arch. Med. Res.* 51(6), 577–581 (2020).
42. Lou Y, Liu L, Yao H *et al.* Clinical outcomes and plasma concentrations of baloxavirmarboxil and favipiravir in COVID-19 patients: an exploratory randomized, controlled trial. *Eur. J. Pharm. Sci.* 157, 105631 (2021).
43. Gao C, Cai Y, Zhang K *et al.* Association of hypertension and antihypertensive treatment with COVID-19 mortality: a retrospective observational study. *Eur. Heart J.* 41(22), 2058–2066 (2020).
44. Li J, Wang X, Chen J *et al.* Association of renin-angiotensin system inhibitors with severity or risk of death in patients with hypertension hospitalized for coronavirus disease 2019 (COVID-19) infection in Wuhan, China. *JAMA Cardiol.* 5(7), 825–830 (2020).
45. Marin GH. Facts and reflections on COVID-19 and anti-hypertensives drugs. *Drug Discover. Ther.* 14(2), 105–106 (2020).
46. Zhang H, Penninger JM, Li Y, Zhong N, Slutsky AS. Angiotensin-converting enzyme 2 (ACE2) as a SARS-CoV-2 receptor: molecular mechanisms and potential therapeutic target. *Intensive Care Med.* 46(4), 586–590 (2020).
47. Cheng H, Wang Y, Wang GQ. Organ-protective effect of angiotensin-converting enzyme 2 and its effect on the prognosis of COVID-19. *J. Med. Virol.* 92(7), 726–730 (2020).
48. Gurwitz D. Angiotensin receptor blockers as tentative SARS-CoV-2 therapeutics. *Drug Dev. Res.* 81(5), 537–540 (2020).
49. Waheed AA, Ablan SD, Soheilian F *et al.* Inhibition of human immunodeficiency virus type 1 assembly and release by the cholesterol-binding compound amphotericin B methyl ester: evidence for Vpu dependence. *J. Virol.* 82(19), 9776–9781 (2008).
50. Kim C, Kang H, Kim DE *et al.* Antiviral activity of micafungin against enterovirus 71. *Virol. J.* 13, 99 (2016).
51. Xu F, Zhao X, Hu S *et al.* Amphotericin B inhibits enterovirus 71 replication by impeding viral entry. *Sci. Rep.* 9(6), 33150 (2016).
52. Andreani J, Le Bideau M, Dufflot I *et al.* *In vitro* testing of combined hydroxychloroquine and azithromycin on SARS-CoV-2 shows synergistic effect. *Microb. Pathog.* 145, 104228 (2020).
53. Wang K, Chen W, Zhou YS *et al.* SARS-CoV-2 invades host cells via a novel route: CD147-spike protein. *bioRxiv* doi:10.1101/2020.03.14.988345 (2020) (Epub ahead of print).
54. Wang S, Liu C, Liu X *et al.* Effects of matrix metalloproteinase inhibitor doxycycline and CD147 antagonist peptide-9 on gallbladder carcinoma cell lines. *Tumour Biol.* 39(10), 1010428317718192 (2017).
55. Yuan L, Yu J, Huang Y *et al.* Antibiotic fidaxomicin is an RdRp inhibitor as a potential new therapeutic agent against Zika virus. *BMC Med.* 18(1), 204 (2020).
56. Azarmi S, Roa W, Lobenberg R. Current perspectives in dissolution testing of conventional and novel 56 dosage forms. *Int. J. Pharm.* 328(1), 12–21 (2007).
57. Shekhawat PB, Pokharkar VB. Understanding *peroral* absorption: regulatory aspects and contemporary approaches to tackling solubility and permeability hurdles. *Acta Pharm. Sin. B* 7(3), 260–280 (2017).
58. Kimura T, Higaki K. Gastrointestinal transit and drug absorption. *Biol. Pharm. Bull.* 25(2), 149–164 (2002).
59. Tran N. Blood–brain barrier. In: *Encyclopedia of Clinical Neuropsychology*. Kreutzer JS, DeLuca J, Caplan B (Eds). Springer, NY, USA (2011).
60. Amin ML. P-glycoprotein inhibition for optimal drug delivery. *Drug Target Insights* 7, 27–34 (2013).
61. Robey RW, Pluchino KM, Hall MD *et al.* Revisiting the role of ABC transporters in multidrug-resistant cancer. *Nat. Rev. Cancer* 18(7), 452–464 (2018).
62. Mohamed A, El-Kadi AOS. P-glycoprotein effects on drugs pharmacokinetics and drug–drug interactions and their clinical implications. *Libyan J. Pharm. Clin. Pharmacol.* 1, 48154 (2012).
63. Palleria C, Paolo AD, Giofre C *et al.* Pharmacokinetic drug–drug interaction and their implication in clinical management. *J. Res. Med. Sci.* 18(7), 601–610 (2013).
64. Al Wasidi AS, Hassan AS, Naglah AM. *In vitro* cytotoxicity and druglikeness of pyrazolines and pyridines bearing benzofuran moiety. *J. App. Pharma. Sci.* 10(4), 142–148 (2020).
65. Kujawski J, Popielarska H, Myka A *et al.* The log P parameter as a molecular descriptor in the computer-aided drug design: an overview. *Comput. Methods Sci. Technol.* 18(2), 81–88 (2012).